

STUDIES ON GRAVITATIONAL WAVES FROM COMPACT BINARIES

A dissertation submitted in partial fulfilment for the award of the
Masters degree in Physics

Done by

Saikruba. K

Registration No. : 34314006

under the supervision of

Dr. R. Radhakrishnan

*Department of Theoretical Physics,
University of Madras*



Department of Theoretical physics,
University of Madras, Guindy
Chennai-600 025

MAY 2016

BONAFIDE CERTIFICATE

This is to certify that the dissertation entitled **STUDIES ON GRAVITATIONAL WAVES FROM COMPACT BINARIES** is submitted by **SAIKRUBA .K**, in partial fulfillment of the requirements for award of Master of Science degree in Physics, is a bonafide record of work done by the candidate under my guidance and supervision at Department of Theoretical Physics, University of Madras.

Dr. R.Radhakrishnan
Assistant Professor
Department of Theoretical Physics
University of Madras
Guidny-600025,India

ACKNOWLEDGEMENT

I express my deep sense of gratitude to my guide Dr.R.Radhakrishnan for giving me the opportunity to carry out my post graduation dissertation work under his guidance. His clear guidance, encouraging words and patience helped me finish this project.

I would like to thank Dr.Rita John, Head of the department, Department of Theoretical physics, University of Madras, for encouraging us to take up research career and providing us with all the help and support we could ever have throughout the course.

I would like to express my sincere gratitude to Dr.Vytheeswaran, Assistant professor, Department of Theoretical physics, University of Madras from whom I have learnt a lot and will always be grateful. His advices for career and life are precious.

I would like to thank my family for their support and love. I would like to thank my friend Prasad Ravichandran for the cheerful support and encouragement.

Contents

Introduction	4
1 Space-time and Einstein's equation	5
2 Linearized Gravity	11
2.1 Weak field limit and metric perturbation	11
2.2 Linearization of Einsteins equations	12
2.3 Static weak field : Newtonian Gravity	14
2.4 Changing weak field : Gravitational radiation	15
2.5 Polarization and effect on test particles	18
3 Generation of Gravitational waves	21
3.1 Possible sources	21
3.2 Perturbation tensor in terms of source parameters	22
4 Gravitational waves from binaries	26
4.1 Circular orbit	28
4.2 Elliptical orbit	34
5 Newtonian chirp from inspiraling binaries	43
5.1 Newtonian Chirp	43
5.2 Binaries at galactic center	44
5.3 Supermassive black holes and slowly orbiting systems	48
5.4 GW150914	51
5.5 Amplitude spectral density	52
5.6 Data analysis from waveform	54
6 Gravitational waves from accreting millisecond pulsars	58
6.1 Neutron star spin down and spin up	58
6.2 Quadrupole asymmetry	61
6.3 Accretion torque and GW torque equilibrium	65
Conclusion	68
Reference	69

Introduction

Gravitational waves are the predictions of General relativity. Theoretical investigation in the past century brought out various scenarios in which gravitational waves could be produced, namely inspiral-merger-ringdown of binaries, spinning neutron stars, accreting neutron stars, bursts, stochastic background etc. Observational evidences in certain accreting binaries indicated possibility of energy loss due to gravitational waves, but they could never be studied completely to check whether such systems evolve as per general relativity or not. In 1991 Hulse and Taylor found that the period of PSR B1913+16 binary pulsar changes in agreement with general relativity. The first search for direct detection of gravitational waves was done by J. Weber using his bar detector. Laser interferometer detectors ground-based and space-based have provided a suitable way to observe gravitational waves, but it has its own limitations. LIGO detector collected data from 2002 to 2010 but no gravitational waves were observed. After its upgrade the detectors began collecting data in 2015 where the first direct observation of gravitational waves was seen and the detection event was named GW150914. The study of GW150914 revealed that it corresponds to collision and merger of two black holes in a binary to form a new black hole. Future detections can be seen in aLIGO, VIRGO, LISA, Einstein telescope, Cosmic explorer, Pulsar Timing Array, KAGRA and others.

The aim of this dissertation work is to understand the theoretical aspects of gravitational waves, carry out a theoretical study of inspiraling compact binaries and accreting neutron star systems as sources of gravitational waves, and also to analyze the possible distances and possible sources parameters which could be observed in future in gravitational wave regime on Earth. Starting few chapters is review of mathematical preliminaries and theoretical foundations, while the later part of dissertation is devoted to the study of inspiraling compact binaries and accreting neutron star systems.

Chapter 1

Space-time and Einstein's equation

Einstein's general relativity describes gravity as curvature of space-time. The laws of physics are independent of the coordinate system used to study it. A equation written in a given coordinate system has to remain in the same form in all coordinate system. This implies that if A, B, C, D and λ are quantities in a given coordinate system and in a any other coordinate system the corresponding quantities are A', B', C', D' and λ' , and if $A = B + C - \lambda D$ is the equation in a coordinate system then it must be $A' = B' + C' - \lambda' D'$ in any other coordinate system. It does not mean that $A' = A, B' = B, C' = C, D' = D$ and $\lambda' = \lambda$. Different quantities transform in different way in going from one coordinate system to other but the form of the equation should remain the same. This is very essential as laws of physics are independent of the coordinate system chosen and this very need requires notions of tensors and their properties.

If we have a 4-D space-time coordinate system with coordinates x^α then for any other coordinate system with coordinates x'^α there exists a transformation relation $x^\mu \rightarrow x'^\nu$. In general each coordinate x'^ν is a function of all coordinates x^μ and vice-versa.

It implies $x'^0 = x'^0(x^0, x^1, x^2, x^3)$, $x'^1 = x'^1(x^0, x^1, x^2, x^3)$, $x'^2 = x'^2(x^0, x^1, x^2, x^3)$, and $x'^3 = x'^3(x^0, x^1, x^2, x^3)$. Hence can be written as-

$$x'^\nu = x'^\nu(x^0, x^1, x^2, x^3)$$

$$\Rightarrow x'^\nu = x'^\nu(x^\mu)$$

Hence the coordinate differentials are related as

$$dx'^\nu = \frac{\partial x'^\nu}{\partial x^\mu} dx^\mu \quad (1.1)$$

We briefly describe scalars, covariant and contravariant components of vectors and tensors[24, 2] before outlining various aspects of general relativity and eventually the Einstein's equation[2, 17]

Scalar

A single component quantity ϕ which under coordinate transformation transforms to ϕ' such that

$$\phi' = \phi \quad (1.2)$$

then it is called as a scalar. It remains same in all coordinate system.

Covariant and contravariant vector

A quantity having four components A^μ where $\mu = 0, 1, 2, 3$ if under a general coordinate transformation, transforms to A'^μ which can be related by the transformation equation

$$A'^\mu = \frac{\partial x'^\mu}{\partial x^\nu} A^\nu \quad (1.3)$$

then it is called as contravariant vector.

A quantity having four components A_μ where $\mu = 0, 1, 2, 3$ if under a general coordinate transformation, transforms to A'_μ which can be related by the transformation equation

$$A'_\mu = \frac{\partial x^\nu}{\partial x'^\mu} A_\nu \quad (1.4)$$

then it is called as a covariant vector.

Tensors

If a quantity has 16 components $A^{\mu\nu}$ where $\mu, \nu = 0, 1, 2, 3$ and transforms as

$$A'^{\mu\nu} = \frac{\partial x'^\mu}{\partial x^\alpha} \frac{\partial x'^\nu}{\partial x^\beta} A_{\alpha\beta} \quad (1.5)$$

then it is called as contravariant tensor of rank-2 . If it has components $A_{\mu\nu}$ where $\mu, \nu = 0, 1, 2, 3$ and transforms as

$$A'_{\mu\nu} = \frac{\partial x^\alpha}{\partial x'^\mu} \frac{\partial x^\beta}{\partial x'^\nu} A_{\alpha\beta} \quad (1.6)$$

then it is called as covariant tensor of rank-2. If it has components A^μ_ν which transforms as

$$A'^\mu_\nu = \frac{\partial x'^\mu}{\partial x^\alpha} \frac{\partial x^\beta}{\partial x'^\nu} A^\alpha_\beta \quad (1.7)$$

then it is called as mixed tensor of rank-2 with covariant rank 1 and contravariant rank 1.

Space-time

The space-time is defined by metric tensor. Metric tensor reveals about the geometry of space-time and curvature through line element, christoffel symbols and Riemann tensor. A flat space-time is described by Minkowski metric tensor $\eta_{\mu\nu}$. The line element ds between any two nearby

events with coordinates x^μ and $x^\mu + dx^\mu$ is

$$ds^2 = \eta_{\mu\nu} dx^\mu dx^\nu \quad (1.8)$$

where $\mu, \nu = 0, 1, 2, 3$ and Minkowski metric tensor is defined as

$$\eta_{\mu\nu} = \begin{pmatrix} -1 & 0 & 0 & 0 \\ 0 & 1 & 0 & 0 \\ 0 & 0 & 1 & 0 \\ 0 & 0 & 0 & 1 \end{pmatrix} \quad (1.9)$$

In Minkowski space-time the coordinates transform according to Lorentz transformation. The Lorentz transformation matrix is represented by

$$\Lambda = \begin{pmatrix} \gamma & -v\gamma & 0 & 0 \\ -v\gamma & \gamma & 0 & 0 \\ 0 & 0 & 1 & 0 \\ 0 & 0 & 0 & 1 \end{pmatrix} \quad (1.10)$$

The coordinates transforms as

$$x'^\mu = \Lambda^\mu_\nu x^\nu$$

where $\Lambda^\mu_\nu = \frac{\partial x^\mu}{\partial x'^\nu}$. It is important to note that the covariant vectors, contravariant vectors and tensors in Minkowski space transform according to Lorentz transformation.

$$A'_{\mu\nu} = \Lambda^\rho_\mu \Lambda^\sigma_\nu A_{\rho\sigma}$$

which is essentially the same as . The metric $g_{\mu\nu}(x)$ is a generalization of $\eta_{\mu\nu}$ in curved space-time. If we assume that ds^2 is invariant under general coordinate transformation then we have

$$ds^2 = g_{\mu\nu}(x) dx^\mu dx^\nu \rightarrow ds^2 = g'_{\alpha\beta}(x') dx'^\alpha dx'^\beta \quad (1.11)$$

substituting the transformation relation of dx'^α, dx'^β from Eq.(1.1), we can write

$$\begin{aligned} ds^2 &= g_{\mu\nu}(x) \left(\frac{\partial x^\mu}{\partial x'^\alpha} dx'^\alpha \right) \left(\frac{\partial x^\nu}{\partial x'^\beta} dx'^\beta \right) \\ &= g'_{\alpha\beta}(x') dx'^\alpha dx'^\beta \end{aligned} \quad (1.12)$$

Comparing Eq.(1.11) & Eq.(1.12) we get the result

$$g'_{\alpha\beta}(x') = \frac{\partial x^\mu}{\partial x'^\alpha} \frac{\partial x^\nu}{\partial x'^\beta} g_{\mu\nu}(x) \quad (1.13)$$

where $g_{\mu\nu}$ is a second rank covariant tensor. We can use this metric tensor to convert between the covariant and contravariant tensors.

$$A^\mu = g^{\mu\nu}(x)A_\nu \quad (1.14)$$

is a contravariant vector corresponding to the covariant vector A_ν . While we have

$$A_\mu = g_{\mu\nu}(x)A^\nu \quad (1.15)$$

which is a covariant vector corresponding to the contravariant vector A^ν .

Christoffel symbols

There are two types of christoffel symbols or the affine connections. The christoffel symbol of the first kind is defined as

$$[pq, r] = \Gamma_{pq, r} = \frac{1}{2} \left(\frac{\partial g_{pr}}{\partial x^q} + \frac{\partial g_{qr}}{\partial x^p} - \frac{\partial g_{pq}}{\partial x^r} \right) \quad (1.16)$$

The christoffel symbol of the second kind is defined as

$$\Gamma_{pq}^s = g^{sr} [pq, r] \quad (1.17)$$

Christoffel symbols can be found using the metric tensor. For Minkowski space-time the metric tensor is independent of coordinates hence all christoffel symbols are zero. In flat space-time all christoffel symbols are zero.

Covariant derivative

Using the definition of affine connection, we can obtain the expression for covariant derivative of a contravariant tensor A^μ is as follows,

$$A^\mu; \nu = A^\mu, \nu + \Gamma_{\nu\alpha}^\mu A^\alpha \quad (1.18)$$

where

$$A^\mu, \nu \equiv \frac{\partial A^\mu}{\partial x^\nu} \quad (1.19)$$

The transformation of christoffel symbols under the general coordinate transformation is

$$\Gamma_{\alpha\beta}^\mu(x^\lambda) \rightarrow \Gamma'_{\alpha\beta}{}^\mu(x'^\lambda) = \frac{\partial x'^\mu}{\partial x^\nu} \frac{\partial x^\sigma}{\partial x'^\alpha} \frac{\partial x^\gamma}{\partial x'^\beta} \Gamma_{\sigma\gamma}^\nu(x^\lambda) + \frac{\partial x'^\mu}{\partial x^\nu} \frac{\partial^2 x^\nu}{\partial x'^\alpha \partial x'^\beta} \quad (1.20)$$

The second term in the right hand side of Eq.(1.20) indicates that christoffel symbol is not a tensor, but this term ensures that covariant derivative of a tensor results in a tensor. In flat space-time covariant derivative reduces to partial derivatives.

Geodesic equation

A geodesic is a curve of extremal length between any two points. In general relativity in the absence of external force objects move along the geodesics. The equation of a geodesic is

$$\frac{d^2 x^\alpha}{d\lambda^2} + \Gamma^\alpha_{\mu\beta} \frac{dx^\mu}{d\lambda} \frac{dx^\beta}{d\lambda} = 0 \quad (1.21)$$

where λ is the affine parameter on the geodesic. It can be chosen to be proper time for $m \neq 0$ cases

$$\frac{d^2 x^\alpha}{d\tau^2} + \Gamma^\alpha_{\mu\beta} \frac{dx^\mu}{d\tau} \frac{dx^\beta}{d\tau} = 0 \quad (1.22)$$

Riemann curvature tensor

The Riemann curvature tensor $R^\mu_{\nu\alpha\beta}$ represents how curved is the space-time geometry, and is constructed using the christoffel symbol and its derivatives in the following way,

$$R^\mu_{\nu\alpha\beta} = \frac{\partial \Gamma^\mu_{\nu\beta}}{\partial x^\alpha} - \frac{\partial \Gamma^\mu_{\nu\alpha}}{\partial x^\beta} + \Gamma^\mu_{\sigma\alpha} \Gamma^\sigma_{\nu\beta} - \Gamma^\mu_{\sigma\beta} \Gamma^\sigma_{\nu\alpha} \quad (1.23)$$

it satisfies

$$R^\mu_{\nu\alpha\beta} = -R^\mu_{\nu\beta\alpha} \quad (1.24)$$

Space-time is said to be flat if its Riemann tensor vanishes (since christoffel symbols are zero), otherwise it is curved. We can obtain a symmetric second rank tensor called the Ricci tensor by contracting the Riemann tensor,

$$R_{\nu\beta} = R^\mu_{\nu\mu\beta} = R_{\beta\nu} \quad (1.25)$$

By further contracting we get the Ricci scalar which is

$$R = g^{\mu\nu} R_{\mu\nu} \quad (1.26)$$

Since $R_{\mu\nu\alpha\beta} = g_{\mu\lambda} R^\lambda_{\nu\alpha\beta}$ all the symmetry of the curvature tensor are

$$R_{\mu\nu\alpha\beta} = -R_{\mu\nu\beta\alpha} = -R_{\nu\mu\alpha\beta} = R_{\alpha\beta\mu\nu} \quad (1.27)$$

Einstein's equation

Einstein gave his field equations in 1915. Einstein's equation is

$$G_{\mu\nu} = R_{\mu\nu} - \frac{1}{2} g_{\mu\nu} R = \frac{8\pi G}{c^4} T_{\mu\nu} \quad (1.28)$$

where $\mu, \nu = 0, 1, 2, 3$. The L.H.S of Einstein's equation is $G_{\mu\nu}$ which is called as the Einstein's tensor and it can be constructed from christoffel symbols using the metric tensor. The R.H.S consists of stress-energy tensor (also called energy-momentum tensor) whose components are :

1. T^{00} = Energy density = ρ
2. T^{0i} = Energy flux
3. T^{i0} = Momentum density
4. T^{ij} = Momentum flux (Also called stress)

A mass-energy configuration produces distortion in space-time around it, which results in curved space-time. Einstein's equation is a set of 16 equations out of which 10 are independent. Only for symmetrical and special cases solution for Einstein's equation has been obtained.

Chapter 2

Linearized Gravity

We obtain the weak field limit of Einstein's field equation. The weak field limit can give two possibilities, a static weak-field and a changing weak-field. The static weak field leads to Newtonian gravity whereas the changing weak-field leads to gravitational waves. The weak field limit of Einstein's is described in detail from Ref[17].

2.1 Weak field limit and metric perturbation

The Einsteins equation is given by

$$G_{\mu\nu} = R_{\mu\nu} - \frac{1}{2} g_{\mu\nu} R = \frac{8\pi G}{c^4} T_{\mu\nu} \quad (2.1)$$

A weak gravitational field can be considered as a small “perturbation” on the flat Minkowski metric and is associated with space-time which is slightly curved. The metric of such a region is of the form

$$g_{\mu\nu} = \eta_{\mu\nu} + h_{\mu\nu}, \quad |h_{\mu\nu}| \ll 1 \quad (2.2)$$

where the nature of perturbation $h_{\mu\nu}$ plays a crucial role. It turns out that perturbation is a tensor and a trace-reverse can be written for it. Gauge transformation exists for both the perturbation tensor and trace-reverse. This section highlights these details. Under Lorentz transformation the coordinates changes and the metric transforms as $g_{\mu\nu} \rightarrow g'_{\mu\nu}(x')$, where

$$g'_{\mu\nu}(x') = \frac{\partial x^\rho}{\partial x'^\mu} \frac{\partial x^\sigma}{\partial x'^\nu} g_{\rho\sigma}(x) \quad (2.3)$$

$$\begin{aligned} g'_{\mu\nu}(x') &= \Lambda_\mu^\rho \Lambda_\nu^\sigma g_{\rho\sigma} \\ &= \Lambda_\mu^\rho \Lambda_\nu^\sigma \eta_{\rho\sigma} + \Lambda_\mu^\rho \Lambda_\nu^\sigma h_{\rho\sigma}(x) \\ g'_{\mu\nu}(x') &= \eta'_{\mu\nu} + h'_{\mu\nu}(x'), \end{aligned}$$

We can infer that

$$h'_{\mu\nu}(x') = \Lambda_\mu^\rho \Lambda_\nu^\sigma h_{\rho\sigma}(x) \quad (2.4)$$

which implies that the perturbation transforms as a tensor under Lorentz transformation. Now consider an arbitrary small transformation $x^\mu \rightarrow x'^\mu$

$$\begin{aligned} x'^\mu &= x^\mu + \xi^\mu(x), & |\partial_\mu \xi_\nu| &\leq |h_{\mu\nu}| \\ \Rightarrow x^\mu &= x'^\mu - \xi^\mu(x) \end{aligned} \quad (2.5)$$

We differentiate to obtain $\frac{\partial x^\rho}{\partial x'^\mu} = \delta_\mu^\rho - \partial_\mu \xi^\rho$ and $\frac{\partial x^\sigma}{\partial x'^\nu} = \delta_\nu^\sigma - \partial_\nu \xi^\sigma$. We substitute this in the metric transformation Eq.(2.3)

$$\begin{aligned} g'_{\mu\nu}(x') &= \frac{\partial x^\rho}{\partial x'^\mu} \frac{\partial x^\sigma}{\partial x'^\nu} g_{\rho\sigma}(x) \\ &= (\delta_\mu^\rho - \partial_\mu \xi^\rho)(\delta_\nu^\sigma - \partial_\nu \xi^\sigma) g_{\rho\sigma} \\ &= (\delta_\mu^\rho - \partial_\mu \xi^\rho)(\delta_\nu^\sigma - \partial_\nu \xi^\sigma)(\eta_{\rho\sigma} + h_{\rho\sigma}) \\ g'_{\mu\nu} &= \eta_{\mu\nu} - \partial_\nu \xi_\mu - \partial_\mu \xi_\nu + h_{\mu\nu} \\ g'_{\mu\nu} &= \eta_{\mu\nu} + h'_{\mu\nu} \end{aligned}$$

where we have

$$h'_{\mu\nu} = h_{\mu\nu} - \xi_{\mu,\nu} - \xi_{\nu,\mu}, \quad |h'_{\mu\nu}| \ll 1 \quad (2.6)$$

The linearized Riemann tensor is invariant under the transformation $h_{\mu\nu} \rightarrow h_{\mu\nu} - \partial_\mu \xi_\nu - \partial_\nu \xi_\mu$. Hence the Ricci tensor, Ricci scalar and eventually the equation of motion is invariant under this transformation and this is called as the Gauge transformation. The transformed perturbation tensor has the old perturbation tensor with some extra quantity. We can define a trace-reverse tensor

$$\bar{h}^{\mu\nu} = h^{\mu\nu} - \frac{1}{2} \eta^{\mu\nu} h \quad (2.7)$$

where $h = \eta_{\alpha\beta} h^{\alpha\beta}$ and $\bar{h} = -h$ (hence called as trace reverse tensor). Under gauge transformation of this trace reverse tensor

$$\begin{aligned} \bar{h}'^{\mu\nu} &= h'^{\mu\nu} - \frac{1}{2} \eta^{\mu\nu} h' \\ &= (h_{\mu\nu} - \xi_{\mu,\nu} - \xi_{\nu,\mu}) - \frac{1}{2} \eta^{\mu\nu} (h - 2\partial_\sigma \xi^\sigma) \\ \bar{h}'^{\mu\nu} &= \bar{h}^{\mu\nu} - \xi_{\mu,\nu} - \xi_{\nu,\mu} + \eta^{\mu\nu} \xi_{,\sigma}^\sigma \end{aligned} \quad (2.8)$$

2.2 Linearization of Einsteins equations

In order to write the Einstein's equation in linearized form, firstly we rewrite the Christoffel symbols, Riemann tensor, Ricci tensor and Ricci Scalar in linearized form

$$\Gamma_{\mu\rho}^\nu = \frac{g^{\nu\lambda}}{2} [\partial_\rho g_{\lambda\mu} + \partial_\mu g_{\lambda\rho} - \partial_\lambda g_{\mu\rho}]$$

we write

$$g_{\mu\nu} = \eta_{\mu\nu} + h_{\mu\nu}$$

and we also know that $\partial\eta_{\mu\nu} = 0$, therefore we have

$$\Gamma_{\mu\rho}^{\nu} = \frac{1}{2}\eta^{\nu\lambda}(\partial_{\rho}h_{\lambda\mu} + \partial_{\mu}h_{\lambda\rho} - \partial_{\lambda}h_{\mu\rho}) \quad (2.9)$$

thus the Reimenn curvature tensor takes the form

$$R_{\mu\rho\sigma}^{\nu} = \partial_{\rho}\Gamma_{\mu\sigma}^{\nu} - \partial_{\sigma}\Gamma_{\mu\rho}^{\nu} + \mathcal{O}(h^2)$$

Finally the covariant Reimenn tensor is defined as

$$R_{\alpha\mu\rho\sigma} = \eta_{\alpha\nu}R_{\mu\rho\sigma}^{\nu}$$

from this we can construct the Ricci tensor by writing

$$R_{\mu\sigma} = \eta^{\alpha\rho}R_{\alpha\mu\rho\sigma}$$

The Ricci scalar R is obtained from the curvature tensor

$$R = \eta^{\mu\sigma}R_{\mu\sigma}$$

Substituting for Christoffel symbols from Eq.(2.9), the Riemann curvature tensor becomes

$$R_{\mu\rho\sigma}^{\nu} = \frac{1}{2}(\partial_{\rho}\partial_{\mu}h_{\sigma}^{\nu} + \partial_{\sigma}\partial^{\nu}h_{\mu\rho} - \partial_{\rho}\partial^{\nu}h_{\mu\sigma} - \partial_{\sigma}\partial_{\mu}h_{\rho}^{\nu}) \quad (2.10)$$

by contracting we can get the Ricci tensor

$$R_{\nu\sigma} = \frac{1}{2}(\partial_{\sigma}\partial_{\nu}h + \square h_{\nu\sigma} - \partial_{\sigma}\partial_{\nu}h_{\sigma}^{\rho} - \partial_{\rho}\partial_{\nu}h_{\sigma}^{\rho}) \quad (2.11)$$

By contracting we obtain the Ricci scalar as

$$R = \square h - \partial\rho\partial_{\lambda}h^{\rho\lambda} \quad (2.12)$$

By substituting in Einstein equation we get

$$\partial_{\sigma}\partial_{\nu}h + \square h_{\nu\sigma} - \partial_{\sigma}\partial_{\nu}h_{\sigma}^{\rho} - \partial_{\rho}\partial_{\nu}h_{\sigma}^{\rho} - \eta_{\nu\sigma}(\square h - \partial\rho\partial_{\lambda}h^{\rho\lambda}) = -\frac{16\pi G}{c^4}T_{\nu\sigma} \quad (2.13)$$

Equation can be greatly simplified if we introduce the so-called *trace-reverse* tensor

$$\bar{h}^{\mu\nu} = h^{\mu\nu} - \frac{1}{2}\eta^{\mu\nu}h, \quad (2.14)$$

Using the trace-reverse tensor we get

$$\square \bar{h}_{\nu\sigma} + \eta_{\nu\sigma} \partial^\rho \partial^\lambda \bar{h}_{\rho\lambda} - \partial^\rho \partial_\nu \bar{h}_{\rho\sigma} - \partial^\rho \partial_\sigma \bar{h}_{\rho\nu} = -\frac{16\pi G}{c^4} T_{\nu\sigma} \quad (2.15)$$

To further simplify we can impose the Lorenz gauge (also denoted in the literature as harmonic or De Donder gauge)

$$\partial_\nu \bar{h}^{\mu\nu} = 0,$$

and obtain the equation satisfied by trace reversed metric tensor as

$$\square \bar{h}_{\mu\nu} = -\frac{16\pi G}{c^4} T_{\mu\nu} \quad (2.16)$$

Einstein's equation in weak field limit has led to the above equation in terms of perturbation. The weak field can be static or time changing. The solution to above equation differs for static and time changing field. Both the static and time changing field we discuss in next section.

2.3 Static weak field : Newtonian Gravity

We assume that the T_{00} component which is rest-mass energy is dominant that other components of $T_{\mu\nu}$. This also implies that \bar{h}_{00} is larger than other components of $\bar{h}_{\mu\nu}$. Trace of perturbation tensor, $h = -\bar{h}$ as $\bar{h}_{\mu\nu}$ is trace-reverse of $h_{\mu\nu}$.

$$h = -\bar{h} = -\eta^{\mu\nu} \bar{h}_{\mu\nu} = \sum -\eta^{\mu\nu} \bar{h}_{\mu\nu} \quad (2.17)$$

Using the values of Minkowski metric tensor and keeping \bar{h}_{00} as larger and neglecting other components of $\bar{h}_{\mu\nu}$ we get [18]

$$h = -\eta^{00} \bar{h}_{00} = \bar{h}_{00} \quad (2.18)$$

From definition, $\bar{h}_{\mu\nu} = h_{\mu\nu} - \frac{1}{2} \eta_{\mu\nu} h$

$$\begin{aligned} \bar{h}_{00} &= h_{00} - \frac{1}{2} \eta_{00} h = h_{00} - \frac{1}{2} \eta_{00} \bar{h}_{00} \\ \bar{h}_{00} - \frac{1}{2} \bar{h}_{00} &= h_{00} \\ \bar{h}_{00} &= 2h_{00} \end{aligned} \quad (2.19)$$

With the $\mu, \nu = 0$ one of the Einstein's equation is

$$\square \bar{h}_{00} = -\frac{16\pi G}{c^4} T_{00} \quad (2.20)$$

Substituting for \bar{h}_{00} and T_{00} we get,

$$\square(2h_{00}) = -\frac{16\pi G}{c^4} (\rho c^2)$$

but for static field $\frac{1}{c^2} \frac{\partial^2 h_{00}}{\partial t^2} = 0$ in D'Alembertian which gives

$$-\nabla^2 h_{00} = -\frac{8\pi G}{c^2} \rho$$

By defining $h_{00} = \frac{2\phi}{c^2}$ we get

$$\nabla^2 \phi = 4\pi G \rho \quad (2.21)$$

which is the Newton's equation for gravity[18].

2.4 Changing weak field : Gravitational radiation

We now consider changing fields[17] , for a source free region we have $T_{\mu\nu} = 0$ thus the wave equation takes the homogeneous form

$$\square \bar{h}_{\mu\nu} = 0 \quad (2.22)$$

but for changing field $\frac{1}{c^2} \frac{\partial^2 \bar{h}_{\mu\nu}}{\partial t^2} \neq 0$ in D'Alembertian which gives the wave equation

$$\frac{1}{c^2} \frac{\partial^2 \bar{h}_{\mu\nu}}{\partial t^2} + \nabla^2 \bar{h}_{\mu\nu} = 0 \quad (2.23)$$

This wave equation has its solution of the form

$$\bar{h}_{\mu\nu} = A_{\mu\nu} \exp(\iota k_\alpha x^\alpha) \quad (2.24)$$

where $A_{\mu\nu}$ is a tensor called as Amplitude tensor. It is a rank-2 tensor and k_α is a constant four-vector known as the wave vector. Since $\bar{h}_{\mu\nu}$ is symmetric $A_{\mu\nu}$ is also symmetric. It has 10 independent components. We try to see if solution has to satisfy Lorentz gauge condition what it would imply

$$\partial_\nu \bar{h}^{\mu\nu} = 0,$$

ie.,

$$\partial_\nu A^{\mu\nu} \exp(\iota k_\alpha x^\alpha) = 0$$

therefore we get

$$A^{\mu\nu} k_\nu = 0$$

or

$$A^{\mu 0} k_0 + A^{\mu 1} k_1 + A^{\mu 2} k_2 + A^{\mu 3} k_3 = 0 \quad \mu = 0, 1, 2, 3 \quad (2.25)$$

We get totally 4 relations, this means that the number of independent components is 6. If k is in Z direction then we have $k^\mu = (k, 0, 0, k)$

$$A^{\mu 0} k_0 + A^{\mu 3} k_3 = 0$$

$$A^{\mu 0} k_0 - A^{\mu 3} k_3 = 0$$

$$A^{\mu 0} k - A^{\mu 3} k = 0$$

we get

$$A^{\mu 0} = A^{\mu 3}$$

The independent components of $A_{\mu\nu}$ are A^{00} , A^{01} , A^{02} , A^{11} , A^{12} , A^{22} . The matrix of the amplitude tensor can be written as

$$A^{\mu\nu} = \begin{pmatrix} A^{00} & A^{01} & A^{02} & A^{00} \\ A^{01} & A^{11} & A^{12} & A^{01} \\ A^{02} & A^{12} & A^{22} & A^{02} \\ A^{00} & A^{01} & A^{02} & A^{00} \end{pmatrix}$$

Though we know that there are only six independent components, it is still not clear about what are these components could be, hence we do the gauge transformation

$$\bar{h}'^{\mu\nu} = \bar{h}^{\mu\nu} - \xi_{,\nu}^{\mu} - \xi_{,\mu}^{\nu} + \eta^{\mu\nu} \xi_{,\sigma}^{\sigma}$$

where we must have

$$\square \xi^{\mu} = 0$$

to be satisfied. The possible solution for ξ^{μ} to satisfy this condition is

$$\xi_{\mu} = \epsilon_{\mu} \exp(\iota k_{\beta} x^{\beta}) \quad (2.26)$$

Substituting $\bar{h}_{\mu\nu} = A_{\mu\nu} \exp(\iota k_{\alpha} x^{\alpha})$ and $\xi_{\mu} = \epsilon_{\mu} \exp(\iota k_{\beta} x^{\beta})$ in gauge transformation equation, we get

$$A'^{\mu\nu} = A^{\mu\nu} - i\epsilon^{\mu} k^{\nu} - i\epsilon^{\nu} k^{\mu} + i\eta^{\mu\nu} \epsilon^{\rho} k_{\rho} \quad (2.27)$$

The components of the transformed amplitude tensor are

$$\begin{aligned} A'^{00} &= A^{00} - ik(\epsilon^0 + \epsilon^3) \\ A'^{11} &= A^{11} - ik(\epsilon^0 - \epsilon^3) \\ A'^{01} &= A^{01} - ik\epsilon^1 \\ A'^{12} &= A^{12} \\ A'^{02} &= A^{02} - ik\epsilon^2 \\ A'^{22} &= A^{22} - ik(\epsilon^0 - \epsilon^3) \end{aligned}$$

Still the number of independent components are 6. ξ^{μ} which assisted in gauge transformation has a arbitrary constant ϵ^{μ} . We have freedom to choose this arbitrary constant and by putting appropriate values we can make some of the components go to zero. If we choose the components

of the arbitrary constant as

$$\begin{aligned}
\epsilon^0 &= -i(2A^{00} + A^{11} + A^{22})/4k \\
\epsilon^1 &= -iA^{01}/k \\
\epsilon^2 &= -iA^{01}/k \\
\epsilon^3 &= -i(2A^{00} - A^{11} - A^{22})/4k
\end{aligned}$$

Then the components of the transformed amplitude tensor will become

$$\begin{aligned}
A'^{00} &= 0 \\
A'^{11} &= -A^{22} \\
A'^{01} &= 0 \\
A'^{12} &= A^{12} \\
A'^{02} &= 0
\end{aligned}$$

We can take $A'^{11} = a$ and $A'^{22} = b$, which are the two independent components of the Amplitude tensor

$$A'^{\mu\nu} = \begin{pmatrix} 0 & 0 & 0 & 0 \\ 0 & a & b & 0 \\ 0 & b & -a & 0 \\ 0 & 0 & 0 & 0 \end{pmatrix} \quad (2.28)$$

The gauge transformation is called as transverse traceless gauge (TT gauge) because it results in Amplitude tensor $A_{TT}^{\mu\nu}$ (and eventually h_{TT}^-) which are traceless and can be written as linear combination of two polarization tensor and hence the term transverse.

$$A_{TT}^{\mu\nu} = ae_+^{\mu\nu} + be_\times^{\mu\nu} \quad (2.29)$$

The polarization tensors are defined as TT gauge ensures that in new gauge there exists two polarization and also makes sure that trace reverse perturbation tensor is equal to the perturbation tensor.

$$\begin{aligned}
\bar{h}'^{\mu\nu} &= h'^{\mu\nu} \\
e_+^{\mu\nu} &= \begin{pmatrix} 0 & 0 & 0 & 0 \\ 0 & 1 & 0 & 0 \\ 0 & 0 & -1 & 0 \\ 0 & 0 & 0 & 0 \end{pmatrix}, e_\times^{\mu\nu} = \begin{pmatrix} 0 & 0 & 0 & 0 \\ 0 & 0 & 1 & 0 \\ 0 & 1 & 0 & 0 \\ 0 & 0 & 0 & 0 \end{pmatrix} \quad (2.30)
\end{aligned}$$

2.5 Polarization and effect on test particles

In this section we describe the interaction of a GW with a point particle in the TT gauge[19] . Let us consider a test particle A at rest at time $\tau = 0$. Using the geodesic equation, we have

$$\frac{d^2 x^i}{d\tau^2} \Big|_{\tau=0} = - \left(\Gamma_{\rho\sigma}^i \frac{dx^\rho}{d\tau} \frac{dx^\sigma}{d\tau} \right) \Big|_{\tau=0} \quad (2.31)$$

Because the particle is initially at rest

$$(dx^\mu/d\tau)_{\tau=0} = (c, 0) \quad (2.32)$$

we have $\frac{dx^0}{d\tau} = c$ and $\frac{dx^i}{d\tau} = 0$, putting these values

$$\frac{d^2 x^i}{d\tau^2} \Big|_{\tau=0} = - \left(\Gamma_{00}^i \frac{dx^0}{d\tau} \frac{dx^0}{d\tau} \right) \Big|_{\tau=0} \quad (2.33)$$

where $\Gamma_{00}^i = \frac{1}{2} \eta^{ij} (\partial_0 h_{0j} + \partial_0 h_{j0} - \partial_j h_{00})$. In the TT gauge $h_{00} = 0$ and $h_{0j} = 0$, so $(\Gamma_{00}^i)_{\tau=0} = 0$. Thus, we conclude that in the TT gauge, if at time $\tau = 0$ a particle is at rest then

$$\frac{d^2 x^i}{d\tau^2} = 0 \quad (2.34)$$

A particle at rest before the GW arrives, remains at rest. The coordinates in the TT gauge stretch themselves when the GW arrives so that the coordinate position of the point particles, initially at rest, does not vary. What varies is the proper distance between the two particles and physical effects are monitored by proper distances.

$$ds^2 = g_{\mu\nu}(x) dx^\mu dx^\nu$$

In new gauge we have $g_{\mu\nu} = \eta_{\mu\nu} + \bar{h}_{(TT)\mu\nu}$. We have

$$\begin{aligned} \bar{h}_{TT}^{\mu\nu} &= A_{TT}^{\mu\nu} \exp(ik_\alpha x^\alpha) \\ \bar{h}_{TT}^{\mu\nu} &= (ae_+^{\mu\nu} + be_\times^{\mu\nu}) \exp(ik_\alpha x^\alpha) \end{aligned}$$

The physical solution is obtained by taking the real part of $\bar{h}_{TT}^{\mu\nu}$

$$\bar{h}_{TT}^{\mu\nu} = (ae_+^{\mu\nu} + be_\times^{\mu\nu}) \cos(kx^\alpha) = (ae_+^{\mu\nu} + be_\times^{\mu\nu}) \cos(kz - \omega t) \quad (2.35)$$

Taking $b = 0$ we get

$$\bar{h}_{TT}^{\mu\nu} = ae_+^{\mu\nu} \cos(kz - \omega t) \quad (2.36)$$

Evaluating the components of $h_{TT}^{\mu\nu}$ we get the tensor as

$$h_{TT}^{\mu\nu} = \begin{pmatrix} 0 & 0 & 0 & 0 \\ 0 & a & 0 & 0 \\ 0 & 0 & -a & 0 \\ 0 & 0 & 0 & 0 \end{pmatrix} \cos(kz - \omega t) \quad (2.37)$$

Substituting in ds^2 we get

$$\begin{aligned} ds^2 &= g_{\mu\nu}(x)dx^\mu dx^\nu \\ &= (\eta_{\mu\nu} + \bar{h}_{(TT)\mu\nu})dx^\mu dx^\nu \end{aligned}$$

thus the line element will take the final form

$$ds^2 = -dt^2 + [1 + a\cos(kz - \omega t)]dx^2 + [1 - a\cos(kz - \omega t)]dy^2 + dz^2 \quad (2.38)$$

Its very evident that the proper distance along x direction and y direction changes. The space-time itself stretches and contracts due to the metric perturbation where perturbation is solution of wave equation. In first half cycle metric coefficient of g_{11} expands and while the metric coefficient g_{22} contracts. In second half cycle the metric coefficient g_{22} expands and while the metric coefficient g_{11} . This stretching along x-axis while contraction along y-axis and vice-versa is called as + (Plus) Polarization state.

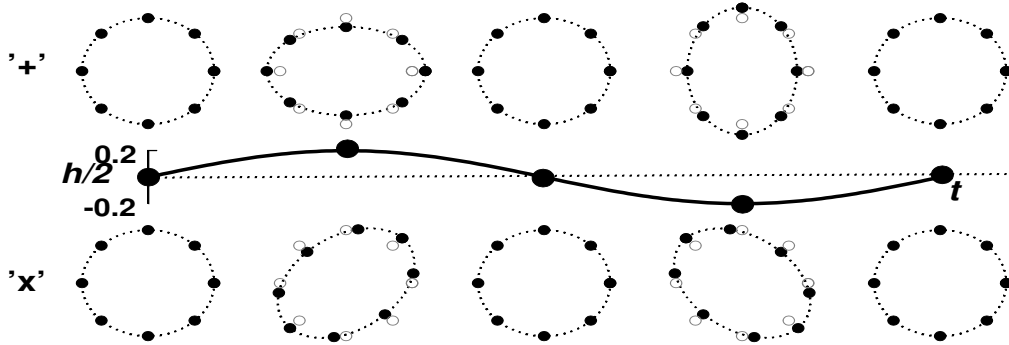


Figure 2.1: Polarization of gravitational waves

Now

$$\bar{h}_{TT}^{\mu\nu} = b e_{\times}^{\mu\nu} \cos(kz - \omega t)$$

Evaluating the components of $h_{TT}^{-\mu\nu}$ we get the tensor as

$$h_{TT}^{-\mu\nu} = \begin{pmatrix} 0 & 0 & 0 & 0 \\ 0 & 0 & b & 0 \\ 0 & b & 0 & 0 \\ 0 & 0 & 0 & 0 \end{pmatrix} \cos(kz - \omega t) \quad (2.39)$$

Substituting in ds^2 we get

$$ds^2 = (\eta_{\mu\nu} + \bar{h}_{(TT)\mu\nu})dx^\mu dx^\nu$$

$$ds^2 = dt^2 + [1 + b\cos(kz - \omega t)]dx dy + dx^2 + [1 + b\cos(kz - \omega t)]dy dx + dy^2 + dz^2 \quad (2.40)$$

In first half cycle metric coefficient of g_{11} and g_{22} expands. In second half cycle the metric coefficient g_{12} and g_{21} contracts. This stretching is in x-y plane and is called as \times (Cross) Polarization state.

Chapter 3

Generation of Gravitational waves

The sources which can produce gravitational waves and the source parameters which decides the gravitational waves produced is presented in this chapter. Whatever be the source, it comes out that in the leading order gravitational waves are produced by changing quadrupole moment.

3.1 Possible sources

The generation of electromagnetic radiation is due to change in electric moments or magnetic moments of a charge-current configuration. The multipole expansion of its electric potential gives several terms each term containing an associated electric moment, namely: electric monopole moment, electric dipole moment, electric quadrupole moment, electric octupole moment etc. The multipole expansion of its magnetic vector potential gives several terms each term containing an associated magnetic moment, namely : magnetic monopole moment, magnetic dipole moment, magnetic quadrupole moment etc.

We have the electric dipole moment $\mathbf{p} = \int \mathbf{r} \rho_e(r) d^3r$ and the magnetic dipole moment $\mathbf{m} = \int \rho_e(r) \mathbf{r} \times \mathbf{v}(r) d^3r$. Electric monopole moment is the total charge and magnetic monopole moment is zero so they don't change with time. Hence they cannot produce electromagnetic radiation. Whereas the other electric and magnetic moments can. The lowest order moment which can change with time to produce electromagnetic radiation is electric dipole moment or magnetic dipole moment. There is no conservation associated with quadrupole, octupole and other higher order moments. Thus change in quadrupole, octupole and higher order moments can also produce electromagnetic waves.

Consider a mass-energy configuration at a distance from origin. The gravitational potential due to this source at any point outside the source can be written down. The Multipole expansion of this potential results in monopole, dipole, quadrupole terms each term containing the associated moment. The total mass-energy, the monopole moment is given by

$$\int \rho(r) d^3r \tag{3.1}$$

The conservation of mass energy implies that its total mass-energy shouldn't change with time.

Hence monopole moment doesn't change with time. The dipole moment is

$$\int r \rho(r) d^3r \quad (3.2)$$

It gives centre of mass-energy. In the centre of mass frame we know that centre of mass-energy remains constant always. Since centre of mass-energy cannot change, the dipole moment doesn't change with time. In centre of mass frame dipole moment doesn't change but does it hold the same in other frames (all frames). It can be shown that there exists dipole moment for other frames given by

$$\int \rho(r) r \times v(r) d^3r \quad (3.3)$$

This gives the total angular momentum of the system. The conservation of angular momentum implies that angular momentum shouldn't change with time. Hence in all frames it can be taken to be valid that there exists no change in dipole moment. The quadrupole moment,

$$I_{ij} = \int r_i r_j \rho(r) d^3r \quad (3.4)$$

There is no conservation law associated to keep the quadrupole moment to be constant over time. Hence quadrupole moment can change with time. The lowest order moment which can produce gravitational waves is quadrupole moment. Thus gravitational wave emission can be expected from binaries, continuous rotating stars with non-axisymmetric lumps, bursts (e.g., asymmetric collapses), and stochastic sources since all these sources have a time varying quadrupole moment [6].

3.2 Perturbation tensor in terms of source parameters

We obtain the perturbation tensor due to quadrupole contribution from a mass-energy configuration with the assumption that the source is non-relativistic and the size of source is much less than the distance from earth. The expression for energy, angular momentum and linear momentum change of the system in terms of quadrupole moment derivatives will be used in next chapter. Different methods to derive exist in literature, we present the outline of method described in Ref[19].

The Einstein equation is given by

$$\square \bar{h}_{\mu\nu} = -\frac{16\pi G}{c^4} T_{\mu\nu}, \quad (3.5)$$

The Einstein equation can be solved using Green's functions. The retarded Green's function is given by

$$G(x - x' | t - t') = -\frac{1}{4\pi} \frac{1}{|\vec{x} - \vec{x}'|} \delta\left(t - \frac{|\vec{x} - \vec{x}'|}{c} - t'\right) \quad (3.6)$$

where δ is the Dirac delta function. The solution for the trace reversed metric perturbation comes out to be

$$\bar{h}_{\mu\nu} = -\frac{16\pi G}{c^4} \int d^4x' G(x-x') T_{\mu\nu}(x') \quad (3.7)$$

where the integral is over the source. To work in TT gauge we create a suitable operator. We consider a $P(\sim n)$ operator which is defined as

$$P_{ij}(\vec{n}) = \delta_{ij} - n_i n_j \quad (3.8)$$

It can remove any components parallel to $\sim n$ in a tensor. We take combination of P operators such that we get a new operator which is also traceless. We use

$$\Lambda_{ij,kl}(\vec{n}) = P_{ik}P_{jl} - \frac{1}{2}P_{ij}P_{kl} \quad (3.9)$$

When the traceless operator act on the metric perturbation, it transforms the metric perturbation to a traceless transverse metric perturbation for any arbitrary propagation direction $\sim n$ of the gravitational waves

$$h_{ij}^{TT} = \Lambda_{ij,kl} h_{kl}$$

this also implies that, even the trace-reverse perturbation tensor can be transformed into traceless transverse

$$\bar{h}_{ij}^{TT} = \Lambda_{ij,kl} \bar{h}_{kl} \quad (3.10)$$

The solution for the trace reversed metric perturbation Eq.(3.7) can be written in TT gauge as

$$\bar{h}_{ij}^{TT}(t, \vec{x}) = \Lambda_{ij,kl}(\vec{n}) \frac{4G}{c^4} \int d^3x' \frac{1}{|\vec{x} - \vec{x}'|} T_{kl} \left(t - \frac{|\vec{x} - \vec{x}'|}{c}; \vec{x}' \right) \quad (3.11)$$

We consider the region far from the source such that the distance to the source r is much larger than the size d of the source. In leading order we can write,

$$|\vec{x} - \vec{x}'| = r - \vec{x}' \cdot \vec{n} + \mathcal{O}(d^2/r), \quad r = \|\vec{x}\|$$

with these assumption the Eq.(3.11) changes as,

$$\bar{h}_{ij}^{TT}(t, \vec{x}) = \frac{4G}{c^4} \frac{1}{r} \Lambda_{ij,kl}(\vec{n}) \int_{|\vec{x}'| < d} d^3x' T_{kl} \left(t - \frac{r}{c} + \frac{\vec{x} \cdot \vec{n}}{c}; \vec{x}' \right) \quad (3.12)$$

We also assume that speeds inside the source are much smaller than the speed of light. In case of binary stars the motion of masses in the binary system must be non-relativistic.

$$\left| \frac{\vec{x}' \cdot \vec{n}}{c} \right| \partial_{t_R} \ll 1$$

where $t_R = t - \frac{r}{c}$ is the retarded time. Now by doing Taylor series expansion of we get,

$$\begin{aligned}\bar{h}_{ij}^{TT} \approx & \frac{1}{r} \frac{4G}{c^4} \Lambda_{ij,kl}(\vec{n}) \left[\int d^3x T^{kl}(t_R, \vec{x}) \right. \\ & + \frac{1}{c} \frac{d}{dt_R} \int d^3x T^{kl}(t_R, \vec{x}) x^m \\ & \left. + \frac{1}{2c^2} n_m n_p \frac{d^2}{dt_R^2} \int d^3x T^{kl}(t_R, \vec{x}) x^m x^p + \dots \right]\end{aligned}\quad (3.13)$$

Eq.(3.13) is like multipole expansion. In the expansion every consecutive term becomes increasingly smaller due to the slow motion of the source. The leading term is,

$$\bar{h}_{ij}^{TT} \approx \frac{1}{r} \frac{4G}{c^4} \Lambda_{ij,kl}(\vec{n}) \int d^3x T^{kl}(t_R, \vec{x}) \quad (3.14)$$

For sources with relativistic velocities, the higher order terms corresponding to octupole, hexadecapole, and other higher order moments has to be considered. It can be shown in terms of mass-energy quadrupole moment $\mathcal{I}^{ij} = \int x^i x^j T^{00}(t, y) d^3x$ a relation exists where,

$$\ddot{\mathcal{I}}^{ij} = 2 \int_V d^3x T^{ij}$$

Thus, general expression for the metric perturbation (in the transverse traceless gauge) in space-time due to a slowly moving and distant source is given by

$$\bar{h}_{ij}^{TT}(t, \vec{x}) = \frac{1}{r} \frac{2G}{c^4} \Lambda_{ij,kl}(\vec{n}) \ddot{\mathcal{I}}^{ij} \left(t - \frac{r}{c} \right) \quad (3.15)$$

Eq.(3.15) can be simplified using a new quantity Q_{ij} called as trace-less quadrupole tensor where

$$Q_{ij} = \mathcal{I}_{ij} - \frac{1}{3} \delta_{ij} \mathcal{I}_{kk} \quad (3.16)$$

It is straight forward to obtain that

$$\bar{h}_{ij}^{TT}(t, \vec{x}) = \frac{1}{r} \frac{2G}{c^4} \ddot{Q}^{ij} \left(t - \frac{r}{c} \right) \quad (3.17)$$

This result is called as **Einstein quadrupole formula**. The total energy radiated by a source in the form of gravitational waves comes out to be

$$\frac{dE}{dt} = \frac{G}{5c^5} \left[\frac{d}{dt} \left(\ddot{Q}_{ij} \right) \frac{d}{dt} \left(\ddot{Q}_{ij} \right) \right] \quad (3.18)$$

Energy is carried away from the source would imply that linear momentum and angular momentum are not conserved. At leading order, the angular momentum radiated away and linear momentum radiated away is

$$\frac{dL^i}{dt} = \frac{2G}{5c^5} \epsilon^{ijk} \left[\ddot{Q}_{jl} \frac{d}{dt} \left(\ddot{Q}_{kl} \right) \right] \quad (3.19)$$

$$\frac{dP^i}{dt} = -\frac{G}{8\pi c^5} \int d\omega \left(\frac{d}{dt} \ddot{Q}_{jk}^{TT} \right) \left(\partial^i \ddot{Q}_{jk}^{TT} \right) \quad (3.20)$$

Eq.(3.17), Eq.(3.18) and Eq.(3.19) serves the essential purpose of obtaining the change in binary parameters like orbital separation, eccentricity, orbital velocity etc. due to the emission of gravitational waves.

Chapter 4

Gravitational waves from binaries

Binary star system consists of two stars orbiting about their common center of mass. The gravitational wave carries both energy and angular momentum from the binary system resulting in orbital parameter changes. We consider a binary system for which we calculate the mass-quadrupole moment in circular and elliptical orbit. Let the mass of two stars be m_1 and m_2 orbiting about a common center of mass in the x-y plane at a distance of r_1 and r_2 respectively. The radial distance between the two stars is

$$r = r_1 + r_2 \quad (4.1)$$

where the orbital radius of the two masses are

$$\mathbf{r}_1 = \frac{m_2}{m_1 + m_2} \mathbf{r} \quad \mathbf{r}_2 = \frac{m_1}{m_1 + m_2} \mathbf{r} \quad (4.2)$$

Assuming that the orbital frequency is ω , the Cartesian coordinates of the two stars can be written as

$$\begin{aligned} x_1 &= r_1 \cos(\omega t) & x_2 &= -r_2 \cos(\omega t) \\ y_1 &= r_1 \sin(\omega t) & y_2 &= -r_2 \sin(\omega t) \end{aligned}$$

The Quadrupole moment tensor of the configuration is

$$\mathcal{I}^{\alpha\beta} = \int X^\alpha X^\beta T^{00}(t, y) d^3X \quad (4.3)$$

The first component of the Energy momentum tensor

$$T^{00} = \rho \quad (4.4)$$

Therefore we re-write Eq.(4.3) as

$$\mathcal{I}^{\alpha\beta} = \int X^\alpha X^\beta \rho dX$$

Since the binary system has discrete mass density (in our case it contains two masses), we have

$$\mathcal{I}^{\alpha\beta} = \sum_i m_i X_i^\alpha X_i^\beta \quad (4.5)$$

where m_i denotes the individual masses and X_i^α denotes coordinates of the star($i = 1$ for the first star or $i = 2$ for the second star). Calculating the non-zero components of the mass quadrupole tensor, for $\alpha = \beta = x$, Eq.(4.5) can be expanded as

$$\mathcal{I}_{xx} = m_1(x_1x_1) + m_2(x_2x_2)$$

Substituting the values for x_1 & x_2 ,

$$\mathcal{I}_{xx} = (m_1r_1^2 + m_2r_2^2) \cos^2 \theta$$

From Eq.(4.2), we get

$$\begin{aligned} \mathcal{I}_{xx} &= \left[m_1 \left(\frac{m_2}{m_1 + m_2} \right)^2 + m_2 \left(\frac{m_1}{m_1 + m_2} \right)^2 \right] r^2 \cos^2 \theta \\ \mathcal{I}_{xx} &= \frac{m_1 m_2}{m_1 + m_2} r^2 \cos^2 \theta \end{aligned} \quad (4.6)$$

Similarly, for $\alpha = \beta = y$, we have

$$\mathcal{I}_{yy} = m_1(y_1y_1) + m_2(y_2y_2)$$

Substituting the values for y_1 and y_2 ,

$$\mathcal{I}_{yy} = (m_1r_1^2 + m_2r_2^2) \sin^2 \theta$$

From Eq.(4.2) we get ,

$$\begin{aligned} \mathcal{I}_{yy} &= \left[m_1 \left(\frac{m_2}{m_1 + m_2} \right)^2 + m_2 \left(\frac{m_1}{m_1 + m_2} \right)^2 \right] r^2 \sin^2 \theta \\ \mathcal{I}_{yy} &= \frac{m_1 m_2}{m_1 + m_2} r^2 \sin^2 \theta \end{aligned} \quad (4.7)$$

Similarly, for $\alpha = x$ and $\beta = y$, we have

$$\mathcal{I}_{xy} = m_1(x_1y_1) + m_2(x_2y_2)$$

Substituting the values of x_1, x_2, y_1 and y_2 we get

$$\mathcal{I}_{xy} = (m_1r_1^2 + m_2r_2^2) \sin \theta \cos \theta$$

From Eq.(4.2) we get ,

$$\begin{aligned}\mathcal{I}_{xy} &= \left[m_1 \left(\frac{m_2}{m_1 + m_2} \right)^2 + m_2 \left(\frac{m_1}{m_1 + m_2} \right)^2 \right] r^2 \sin \theta \cos \theta \\ \mathcal{I}_{xy} &= \frac{m_1 m_2}{m_1 + m_2} r^2 \sin \theta \cos \theta\end{aligned}\tag{4.8}$$

The reduced mass of the system given by

$$\mu = \frac{m_1 m_2}{m_1 + m_2}\tag{4.9}$$

Thus, we have the mass quadrupole tensor as

$$\mathcal{I}_{\alpha\beta} = \mu r^2 \begin{bmatrix} \cos^2 \theta & \sin \theta \cos \theta & 0 \\ \sin \theta \cos \theta & \sin^2 \theta & 0 \\ 0 & 0 & 0 \end{bmatrix}$$

4.1 Circular orbit

We first assume that the two bodies are separated by a large distance and move along a circular orbit. The reduced Quadrupole momentum tensor is given as,

$$Q_{\alpha\beta} = \mathcal{I}_{\alpha\beta} - \frac{1}{3} \delta_{\alpha\beta} \mathcal{I}\tag{4.10}$$

where \mathcal{I} is the trace of the mass quadrupole tensor

$$\mathcal{I} = \mathcal{I}_{xx} + \mathcal{I}_{yy}$$

In chapter 3 we have discussed how the derivative of the reduced quadrupole tensor is essential for calculating different parameters, thus we try to find its derivative up to third order. The non-vanishing components of the reduced quadrupole tensor :

$$Q_{xx} = \mathcal{I}_{xx} - \frac{1}{3} \delta_{xx} \mathcal{I}$$

Substituting for \mathcal{I}_{xx} and the trace of the quadrupole moment, we get

$$\begin{aligned}Q_{xx} &= \mu r^2 \cos^2(\omega t) - \frac{1}{3} \mu r^2 \\ &= \mu r^2 \left[\frac{1 + \cos(2\omega t)}{2} \right] - \frac{1}{3} \mu r^2 \\ &= \frac{\mu r^2}{2} \left[\frac{1}{3} + \cos(2\omega t) \right]\end{aligned}$$

Similarly we need to find the other components,

$$\begin{aligned}
Q_{yy} &= \mathcal{I}_{yy} - \frac{1}{3}\delta_{yy}\mathcal{I} \\
&= \mu r^2 \sin^2(\omega t) - \frac{1}{3}\mu r^2 \\
&= \mu r^2 \left[\frac{1 - \cos(2\omega t)}{2} \right] - \frac{1}{3}\mu r^2 \\
&= \frac{\mu r^2}{2} \left[\frac{1}{3} - \cos(2\omega t) \right]
\end{aligned}$$

$$\begin{aligned}
Q_{xy} &= \mathcal{I}_{xy} - \frac{1}{3}\delta_{xy}\mathcal{I} \\
&= \mu r^2 \cos \theta \sin \theta \\
&= \frac{\mu r^2}{2} \sin(2\omega t)
\end{aligned}$$

$$Q_{yx} = \frac{\mu r^2}{2} \sin(2\omega t)$$

and the corresponding time derivatives are

$$\begin{aligned}
\ddot{Q}_{xx} &= -2\omega\mu r^2 \cos(2\omega t) & \ddot{Q}_{xx} &= 4\omega^3\mu r^2 \sin(2\omega t) \\
\ddot{Q}_{xy} &= -2\omega^2\mu r^2 \sin(2\omega t) & \ddot{Q}_{xy} &= -4\omega^3\mu r^2 \cos(2\omega t) \\
\ddot{Q}_{yx} &= -2\omega^2\mu r^2 \sin(2\omega t) & \ddot{Q}_{yx} &= -4\omega^3\mu r^2 \cos(2\omega t) \\
\ddot{Q}_{yy} &= 2\omega^2\mu r^2 \cos(2\omega t) & \ddot{Q}_{yy} &= -4\omega^3\mu r^2 \sin(2\omega t)
\end{aligned} \tag{4.11}$$

The perturbation is given by Eq.(3.17)

$$h_{ij} = \frac{2}{D}\ddot{Q}_{ij}$$

Where Q_{ij} is a function of $(t - d/c)$ and D is the distance of the binary. Substituting the values from Eq.(4.12),

$$\begin{aligned}
h_{xx} &= -\frac{4\omega^2\mu r^2 \cos(2\omega t)}{D} \\
h_{yy} &= \frac{4\omega^2\mu r^2 \cos(2\omega t)}{D} \\
h_{xy} = h_{yx} &= -\frac{4\omega^2\mu r^2 \sin(2\omega t)}{D}
\end{aligned}$$

Thus we have,

$$h_{ij} = \frac{4\omega^2\mu r^2}{D} \begin{bmatrix} -\cos(2\omega t) & -\sin(2\omega t) & 0 \\ -\sin(2\omega t) & \cos(2\omega t) & 0 \\ 0 & 0 & 0 \end{bmatrix}$$

The radial distance between the binary can be written as

$$r^2 = \frac{M^{2/3}}{\omega^{4/3}}$$

Substituting this value the gravitational wave perturbation can be written as,

$$h_{ij} = \frac{4\omega^{2/3}\mu M^{2/3}}{D} \begin{bmatrix} -\cos(2\omega t) & -\sin(2\omega t) & 0 \\ -\sin(2\omega t) & \cos(2\omega t) & 0 \\ 0 & 0 & 0 \end{bmatrix}$$

By defining $\mathcal{M} = \mu^{3/5} M^{2/5}$, we can write

$$h_{ij} = \frac{4\omega^{2/3}\mathcal{M}^{5/3}}{D} \begin{bmatrix} -\cos(2\omega t) & -\sin(2\omega t) & 0 \\ -\sin(2\omega t) & \cos(2\omega t) & 0 \\ 0 & 0 & 0 \end{bmatrix}$$

$$h(t) = h_+ \begin{bmatrix} -1 & 0 & 0 \\ 0 & 1 & 0 \\ 0 & 0 & 0 \end{bmatrix} + h_\times \begin{bmatrix} 0 & -1 & 0 \\ -1 & 0 & 0 \\ 0 & 0 & 0 \end{bmatrix}$$

The gravitational wave strain due to the two polarizations comes out to be

$$h_+ = \frac{4\omega^{2/3}\mathcal{M}^{5/3}}{D} \cos(2\omega t)$$

$$h_\times = \frac{4\omega^{2/3}\mathcal{M}^{5/3}}{D} \sin(2\omega t)$$

This implies that frequency of gravitational waves is twice the orbital frequency of the binary, i.e one cycle of binary causes two cycles in produced gravitational waves. Hence we can take $\omega = \frac{1}{2}\omega_{gw} = \pi F$, where F is the frequency of the gravitational waves.

$$h_+ = \frac{4 F^{2/3} \pi^{2/3} \mathcal{M}^{5/3}}{D} \cos(2\pi F t) \quad (4.12)$$

$$h_\times = \frac{4 F^{2/3} \pi^{2/3} \mathcal{M}^{5/3}}{D} \sin(2\pi F t) \quad (4.13)$$

From Eqs.(4.12) & (4.13) we can see that the amplitude

$$A(t) = \frac{4 F^{2/3} \pi^{2/3} \mathcal{M}^{5/3}}{D} \quad (4.14)$$

and the phase angle to be $\phi(t) = 2\pi F t$.

Luminosity

The power radiated by the binary system at leading order is given by Eq.(3.17),

$$\begin{aligned}\frac{dE}{dt} &= \frac{-G}{5c^5} \left(\ddot{Q}^{\alpha\beta} \ddot{Q}_{\alpha\beta} \right) \\ &= \frac{-G}{5c^5} [\ddot{Q}^{xx} \ddot{Q}^{xx} + \ddot{Q}^{xy} \ddot{Q}^{xy} + \ddot{Q}^{yy} \ddot{Q}^{yy} + \ddot{Q}^{yx} \ddot{Q}^{yx}]\end{aligned}$$

Substituting the values for the third derivative for the reduced Quadrupole moment from Eq.(4.11),

$$\begin{aligned}\frac{dE}{dt} &= \frac{-G}{5c^5} [\sin^2(2\omega t) + \cos^2(2\omega t) + \sin^2(2\omega t) + \cos^2(2\omega t)] (4\mu r^2 \omega^3)^2 \\ \frac{dE}{dt} &= \frac{-G}{5c^5} (2)(16\mu^2 r^4 \omega^6) = -\frac{32G}{5c^5} \mu^2 r^4 \omega^6\end{aligned}\tag{4.15}$$

The above expression gives the gravitational radiation luminosity of the binary system in circular orbit.

Rate of change of distance between the two stars

The loss of energy decreases the radial separation between the two stars which can be calculated using the total energy of the binary system given as,

$$E = -\frac{G\mu M}{2r}\tag{4.16}$$

where $M = m_1 + m_2$. Differentiating the above Eq. w.r.t time we have

$$\begin{aligned}\frac{dE}{dt} &= \frac{d}{dt} \left[\frac{-G\mu M}{2r} \right] \\ \frac{dE}{dt} &= \frac{G\mu M}{2r^2} \left(\frac{dr}{dt} \right) \\ \dot{r} &= \frac{2r^2}{G\mu M} \left(\frac{dE}{dt} \right)\end{aligned}$$

Substituting the value of rate of change of energy from Eq.(4.15)

$$\dot{r} = \frac{2r^2}{G\mu M} \left(-\frac{32G}{5c^5} \mu^2 r^4 \omega^6 \right)\tag{4.17}$$

We know that the angular velocity is given by ,

$$\omega^2 = \frac{GM}{r^3}$$

Substituting the value of ω in Eq.(4.17),

$$\dot{r} = \frac{-64G^3}{5c^5 r^3} \mu M^2 \quad (4.18)$$

this gives the rate of the distance between the two stars in circular orbit acted upon a common central force.

Merging time

As the binary evolves the frequency and amplitude increases and the orbit shrinks. The instant where the binary merge where the distance between the two stars (we are considering point masses) becomes zero is called as merging time. The period during which amplitude and frequency increases considerably we call it as chirp duration. We can write

$$\frac{dE}{dt} = \frac{dE}{dr} \frac{dr}{dt}$$

therefore,

$$\frac{dE}{dr} = \frac{G\mu M}{2r^2}$$

Rearranging and differentiating with time we have

$$\frac{G\mu M}{2r^2} \left(\frac{dr}{dt} \right) = \frac{dE}{dt}$$

substituting the expression for the rate of change of energy with time from Eq.(4.18) we have,

$$\frac{G\mu M}{2r^2} \left(\frac{dr}{dt} \right) = -\frac{32G}{5c^5} \frac{\mu^2 G^3 M^3}{r^5}$$

$$\frac{1}{2} r^3 dr = -\frac{32G^2}{5c^5} \mu M^2 dt$$

Let r_0 and r be the separation between the binary stars at time t_0 and t respectively.

$$\begin{aligned} \int_{r_0}^r \frac{1}{2} r^3 dr &= -\frac{32G^2}{5c^5} \mu M^2 \int_{t_0}^t dt \\ \left[\frac{r^4}{8} \right]_{r_0}^r &= -\frac{32G^2}{5c^5} \mu M^2 t \Big|_{t_0}^t \\ \frac{(r^4 - r_0^4)}{8} &= -\frac{32G^2}{5c^5} \mu M^2 (t - t_0) \\ r^4 - r_0^4 &= \frac{-256G^2}{5c^5} \mu M^2 (t - t_0) \end{aligned} \quad (4.19)$$

When the binary is merging after a time t , we have $r = 0$ and with $t - t_0 = \tau_m$ as the merging time. Putting this condition in Eq.(4.19) we get,

$$r_0^4 = \frac{256G^2}{5c^5} \mu M^2 \tau_m$$

thus we have the **merging time** as

$$\tau_m = \frac{5c^5 r_0^4}{256G^2 \mu M^2} \quad (4.20)$$

the above expression gives the amount of time taken to merge for a binary in a circular orbit. To give the expression for the distance between the two stars in terms of merging time, we can write Eq.(4.19) as

$$\begin{aligned} \left(\frac{r^4}{r_0^4} - 1 \right) &= \frac{-256G^2}{5c^5 r_0^4} \mu M^2 (t - t_0) \\ \frac{r^4}{r_0^4} &= 1 - \frac{256G^2 \mu M^2}{5c^5 r_0^4} (t - t_0) \\ r^4 &= r_0^4 \left[1 - \frac{(t - t_0)}{\tau_m} \right] \end{aligned}$$

Thus, we have

$$r = r_0 \left[1 - \frac{(t - t_0)}{\tau_m} \right]^{\frac{1}{4}} \quad (4.21)$$

where r_0 is the initial distance between the binary. The gravitational wave emission tends to decrease the period of a binary orbit and hence the size of the binary decreases. Although we will not prove it, the emission of gravitational wave radiation also tends to circularize elliptical orbits.

Gravitational wave frequency

The gravitational wave frequency increases with time as the radial distance between the stars shrinks. The expression for it can be determined using the angular frequency of the binary system given as

$$\omega = 2\pi f$$

where f is the frequency of the binary. Since the gravitational wave frequency comes out to be twice the frequency of the binary system, we have

$$\omega = \pi F \quad (4.22)$$

where F is the frequency of the gravitational waves from the binary system in circular orbit. From Kepler's third law we have,

$$\omega^2 = Mr^{-3} \quad (4.23)$$

substituting the value of r from Eq.(4.21) we have

$$\pi^2 F^2 = Mr_0^{-3} \left[1 - \frac{(t - t_0)}{\tau_m} \right]^{-\frac{3}{4}}$$

$$F^2 = \frac{Mr_0^{-3}}{\pi^2} \left[1 - \frac{(t - t_0)}{\tau_m} \right]^{-\frac{3}{4}}$$

Here we have

$$F_0^2 = \frac{Mr_0^{-3}}{\pi^2}$$

which is the gravitational wave frequency at r_0 where the binary angular frequency is $\omega_0^2 = Mr_0^{-3}$. Therefore we can write

$$F^2 = F_0^2 \left[1 - \frac{(t - t_0)}{\tau_m} \right]^{-3/4}$$

$$F(t) = F_0 \left[1 - \frac{(t - t_0)}{\tau_m} \right]^{-3/8} \quad (4.24)$$

The above expression has the gravitational wave frequency written as a function of time.

Phase angle

$$\phi(t) = 2\pi F t$$

$$\phi(t) = \phi_0 - 2 \left[\frac{1}{(256\pi f_0 \mathcal{M})^{8/3}} - \frac{t}{5\mathcal{M}} \right]^{5/8}$$

$$\phi(t) = \phi_0 - 2 \left[\frac{5\mathcal{M}}{5\mathcal{M} (256\pi f_0 \mathcal{M})^{8/3}} - \frac{t}{5\mathcal{M}} \right]^{5/8}$$

$$\phi(t) = \phi_0 - 2 \left[\frac{\tau_m}{5\mathcal{M}} - \frac{t}{5\mathcal{M}} \right]^{5/8}$$

$$\phi(t) = \phi_0 - 2 \left[\frac{\tau_m - t}{5\mathcal{M}} \right]^{5/8} \quad (4.25)$$

4.2 Elliptical orbit

When the binay orbit posses eccentricity then the formulas of orbital parameter changes are more complicated because quantities like energy radiated and angular momentum radiated will vary from one point to other because all the points are not similar in elliptical orbit, and hence need to be averaged properly over the orbit.

This was done first to lowest order by Peters and Matthews by calculating the energy and angular momentum radiated at lowest (quadrupolar) order, and then determining the change in orbital parameters that would occur if the binary completed a full Keplerian ellipse in its

orbit. They assumed that to lowest order the binary can be taken to move as if it experienced only Newtonian gravity, and integrated the losses along that path [6].

We take the orbital plane to be the x-y plane with the centre of mass at the origin and r be the radial distance between the two stars. We describe the change in binary parameters for elliptical orbit described in Ref[8]. If the line joining the masses makes an angle θ with the x-axis, the orbital equation is

$$r = \frac{a(1 - e^2)}{1 + e \cos \theta} \quad (4.26)$$

where a is the semi-major axis, e is the eccentricity. Differentiating the above equation with respect to time ,

$$\dot{r} = e \sin \theta \left[\frac{m_1 m_2}{a(1 - e^2)} \right]^{\frac{1}{2}}$$

Let $c_1 = e \left[\frac{m_1 m_2}{a(1 - e^2)} \right]^{\frac{1}{2}}$. Therefore we can write

$$\dot{r} = c_1 \sin \theta \quad (4.27)$$

We have

$$\dot{\theta} = \frac{[(m_1 + m_2)a(1 - e^2)]^{\frac{1}{2}}}{r^2}$$

Let $c_2 = [(m_1 + m_2)a(1 - e^2)]^{\frac{1}{2}}$,

$$\dot{\theta} = \frac{c_2}{r^2} \quad (4.28)$$

We find the different quantities which can be used for further calculations, by squaring the Eq.(4.26) we have

$$\frac{1}{r^2} = \frac{(1 + e^2 \cos^2 \theta + 2e \cos \theta)}{a^2(1 - e^2)^2} \quad (4.29)$$

Using c_1 , c_2 and Eq.(4.26) we can write as

$$\mu c_1^2 = \frac{m_1 m_2 e^2}{a(1 - e^2)} \quad (4.30)$$

$$\frac{\mu c_2^2}{r^2} = \frac{m_1 m_2 (1 + e^2 \cos^2 \theta + 2e \cos \theta)}{a(1 - e^2)} \quad (4.31)$$

We need to find the third derivative of the Quadrupole moment to find the different parameters of the system, but we see that for an elliptical orbit both r and θ changes with time. We know that

$$\mathcal{I}_{xx} = \mu r^2 \cos^2 \theta$$

taking the first derivative we get

$$\dot{\mathcal{I}}_{xx} = 2\mu \left(\cos^2 \theta r \dot{r} - r^2 \cos \theta \sin \theta \dot{\theta} \right)$$

From Eq.(4.27) and Eq.(4.28),

$$\dot{\mathcal{I}}_{xx} = 2\mu (c_1 r \sin \theta \cos^2 \theta - c_2 \cos \theta \sin \theta)$$

Taking the derivative of the above Eqn.,

$$\ddot{\mathcal{I}}_{xx} = 2\mu c_1 \left\{ \dot{r} \sin \theta \cos^2 \theta + (r \cos^3 \theta - 2r \cos \theta \sin^2 \theta) \dot{\theta} \right\} - 2\mu c_2 \left\{ -\sin^2 \theta + \cos^2 \theta \right\} \dot{\theta}$$

Substituting the values fro \dot{r} & $\dot{\theta}$, we get

$$\begin{aligned} \ddot{\mathcal{I}}_{xx} &= 2\mu \left\{ c_1^2 \sin^2 \theta \cos^2 \theta + \frac{c_1 c_2}{r} (\cos^3 \theta - 2 \cos \theta \sin^2 \theta) - \frac{c_2^2}{r^2} \cos(2\theta) \right\} \\ \ddot{\mathcal{I}}_{xx} &= 2\mu \left\{ c_1^2 \sin^2 \theta \cos^2 \theta + \frac{c_1 c_2}{r} (\cos \theta - 3 \cos \theta \sin^2 \theta) - \frac{c_2^2}{r^2} \cos(2\theta) \right\} \end{aligned}$$

Substituting the values of the constants μ , c_1 , and c_2

$$\begin{aligned} \ddot{\mathcal{I}}_{xx} &= \frac{2m_1 m_2}{a(1-e^2)} \left\{ e^2 \sin^2 \theta \cos^2 \theta + e(1+e \cos \theta) \cos \theta - 3 \cos \theta \sin^2 \theta e(1+e \cos \theta) \right. \\ &\quad \left. - (1+e \cos \theta)^2 \cos(2\theta) \right\} \\ \ddot{\mathcal{I}}_{xx} &= \frac{2m_1 m_2}{a(1-e^2)} \left\{ e^2 \sin^2 \theta \cos^2 \theta + e \cos \theta + e^2 \cos^2 \theta - 3e \cos \theta \sin^2 \theta - \right. \\ &\quad \left. 3e^2 \cos^2 \theta \sin^2 \theta - \cos(2\theta) - e^2 \cos^2 \theta \cos(2\theta) - 2e \cos \theta \cos(2\theta) \right\} \\ \ddot{\mathcal{I}}_{xx} &= \frac{2m_1 m_2}{a(1-e^2)} \left\{ e^2 \sin^2 \theta \cos^2 \theta + e \cos \theta + e^2 \cos^2 \theta - 3e \cos \theta \sin^2 \theta - 3e^2 \cos^2 \theta \sin^2 \theta - \right. \\ &\quad \left. \cos^2 \theta + \sin^2 \theta - e^2 \cos^4 \theta + e^2 \sin^2 \theta \cos^2 \theta - 2e \cos^3 \theta + 2e \cos \theta \sin^2 \theta \right\} \\ \ddot{\mathcal{I}}_{xx} &= \frac{2m_1 m_2}{a(1-e^2)} \left\{ -e \sin^2 \theta \cos^2 \theta + e \cos \theta + e^2 \cos^2 \theta - e \cos \theta \sin^2 \theta - \right. \\ &\quad \left. \cos^2 \theta + \sin^2 \theta - e^2 \cos^2 \theta + e^2 \cos^2 \theta \sin^2 \theta - 2e \cos \theta + 2e \cos \theta \sin^2 \theta \right\} \\ \ddot{\mathcal{I}}_{xx} &= \frac{2m_1 m_2}{a(1-e^2)} \left\{ -e \cos \theta + e \cos \theta \sin^2 \theta + 1 - 2 \cos^2 \theta \right. \\ \ddot{\mathcal{I}}_{xx} &= \frac{2m_1 m_2}{a(1-e^2)} \left\{ -e \cos \theta (1 - \sin^2 \theta) + 1 - 2 \cos^2 \theta \right\} \end{aligned}$$

Therefore the simplified form is given as

$$\ddot{\mathcal{I}}_{xx} = \frac{2m_1 m_2}{a(1-e^2)} \left\{ -e \cos^3 \theta - 2 \cos^2 \theta + 1 \right\} \quad (4.32)$$

differentiating the above Eqn.,

$$\ddot{\mathcal{I}}_{xx} = \frac{2m_1 m_2}{a(1-e^2)} \left\{ 3e \cos^2 \theta \sin \theta + 4 \cos \theta \sin \theta \right\} \dot{\theta}$$

thus we have the final form of $\ddot{\mathcal{I}}_{xx}$

$$\ddot{\mathcal{I}}_{xx} = \frac{2m_1 m_2}{a(1-e^2)} \left\{ 3e \cos^2 \theta \sin \theta + 2 \sin(2\theta) \right\} \dot{\theta} \quad (4.33)$$

we know that

$$\mathcal{I}_{yy} = \mu r^2 \sin^2 \theta = \mu r^2 (1 - \cos^2 \theta)$$

Let us take

$$\mathcal{I}' = \mu r^2$$

and we have $I_{xx} = \mu r^2 \cos^2 \theta$, thus we can write

$$\mathcal{I}_{yy} = \mathcal{I}' - \mathcal{I}_{xx} \quad (4.34)$$

taking the derivative

$$\dot{\mathcal{I}}' = 2\mu r \dot{r}$$

substituting the value of \dot{r} ,

$$\dot{\mathcal{I}}' = 2\mu c_1 r \sin \theta$$

Taking the derivative of the above Eqn.,

$$\ddot{\mathcal{I}}' = 2\mu c_1 (r \cos \theta \dot{\theta} + \dot{r} \sin \theta)$$

From Eqns. (4.27) & (4.28) ,

$$\ddot{\mathcal{I}}' = 2\mu c_1 \left(\frac{c_2}{r} \cos \theta + c_1 \sin^2 \theta \right)$$

substituting for the constants

$$\begin{aligned} \ddot{\mathcal{I}}' &= \frac{2m_1 m_2}{a(1-e^2)} \{e(1+e \cos \theta) \cos \theta + e^2 \sin^2 \theta\} \\ \ddot{\mathcal{I}}' &= \frac{2m_1 m_2}{a(1-e^2)} \{e \cos \theta + e^2 \cos^2 \theta + e^2 \sin^2 \theta\} \\ \ddot{\mathcal{I}}' &= \frac{2m_1 m_2}{a(1-e^2)} \{e \cos \theta + e^2\} \end{aligned}$$

substituting the above result and the value of \ddot{I}_{xx} from Eq.(4.32), we get

$$\ddot{\mathcal{I}}_{yy} = \frac{2m_1 m_2}{a(1-e^2)} \{e^2 + e \cos \theta + e \cos^3 \theta + \cos^2 \theta - \sin^2 \theta\}$$

differentiating the above equation,

$$\begin{aligned} \ddot{\mathcal{I}}_{yy} &= \frac{2m_1 m_2}{a(1-e^2)} \{-e \sin \theta - 3e \cos^2 \theta \sin \theta - 2 \cos \theta \sin \theta - 2 \cos \theta \sin \theta\} \\ \ddot{\mathcal{I}}_{yy} &= -\frac{2m_1 m_2}{a(1-e^2)} \{3e \cos^2 \theta \sin \theta + e \sin \theta + \sin(2\theta)\} \end{aligned} \quad (4.35)$$

similarly we have,

$$\mathcal{I}_{xy} = \mu r^2 \sin \theta \cos \theta$$

Taking the derivative of the above equation,

$$\begin{aligned}\dot{\mathcal{I}}_{xy} &= 2\mu r \dot{r} \cos \theta \sin \theta + \mu r^2 \cos^2 \theta \dot{\theta} - \mu r^2 \sin^2 \theta \dot{\theta} \\ &= 2\mu r \dot{r} \cos \theta \sin \theta + \mu r^2 \cos(2\theta) \dot{\theta}\end{aligned}$$

substituting the values for

$$\dot{\mathcal{I}}_{xy} = 2\mu c_1 r \cos \theta \sin^2 \theta + \mu c_2 \cos(2\theta)$$

differentiating the above equation,

$$\ddot{\mathcal{I}}_{xy} = 2\mu c_1 \left[\cos \theta \sin^2 \theta \ddot{r} + 2\mu c_1 r \sin \theta \cos^2 \theta \dot{\theta} - 2\mu c_1 r \sin^3 \theta \dot{\theta} \right] - 2\mu c_2 \sin(2\theta) \dot{\theta}$$

substituting the values of \dot{r} and $\dot{\theta}$,

$$\begin{aligned}\ddot{\mathcal{I}}_{xy} &= 2\mu \left\{ c_1^2 \sin^3 \theta \cos \theta + \frac{2c_1 c_2}{r} \sin \theta \cos^2 \theta - \frac{c_1 c_2}{r} \sin^3 \theta - \frac{c_2^2}{r^2} \sin(2\theta) \right\} \\ &= 2\mu \left\{ \frac{3c_1 c_2}{r} \sin \theta \cos^2 \theta + c_1^2 \sin^3 \theta \cos \theta - \frac{c_1 c_2}{r} \sin \theta - \frac{c_2^2}{r^2} \sin(2\theta) \right\}\end{aligned}$$

substituting,

$$\begin{aligned}\ddot{\mathcal{I}}_{xy} &= \frac{2m_1 m_2}{a(1-e^2)} \{ 3e(1+e \cos \theta) \cos \theta \sin^2 \theta + e^2 \sin^3 \theta \cos \theta - e(1+e \cos \theta) \sin \theta \\ &\quad - (1+e \cos \theta)^2 \sin(2\theta) \} \\ \ddot{\mathcal{I}}_{xy} &= \frac{2m_1 m_2}{a(1-e^2)} \{ 3e \cos^2 \theta \sin \theta + -3e^2 \cos^3 \theta \sin \theta + e^2 \cos \theta \sin^3 \theta - e \sin \theta - e^2 \sin \theta \cos \theta \\ &\quad - 2 \sin \theta \cos \theta - 2e^2 \cos^3 \theta \sin \theta - 4e \cos^2 \theta \sin \theta \} \\ \ddot{\mathcal{I}}_{xy} &= -\frac{2m_1 m_2}{a(1-e^2)} \{ e \cos^2 \theta \sin \theta + e \sin \theta + 2 \sin \theta \cos \theta \} \quad (4.36)\end{aligned}$$

differentiating

$$\begin{aligned}\ddot{\mathcal{I}}_{xy} &= -\frac{2m_1 m_2}{a(1-e^2)} \{ -2e \cos \theta \sin^2 \theta + e \cos^3 \theta + e \cos \theta + 2 \cos^2 \theta - 2 \sin^2 \theta \} \dot{\theta} \\ \ddot{\mathcal{I}}_{xy} &= -\frac{2m_1 m_2}{a(1-e^2)} \{ 3e \cos^3 \theta - e \cos \theta + 2 \cos(2\theta) \} \quad (4.37)\end{aligned}$$

Power radiated

The power radiated by a gravitational source is given by Eq.(3.17),

$$\begin{aligned}
\frac{dE}{dt} &= -\frac{1}{5} \ddot{Q}_{\beta\gamma} \ddot{Q}^{\beta\gamma} \\
&= -\frac{1}{5} \left(\ddot{I}_{\beta\gamma} \ddot{I}^{\beta\gamma} - \frac{1}{3} \ddot{I}^2 \right) \\
&= -\frac{1}{5} \left(\ddot{I}_{xx}^2 + 2\ddot{I}_{xy}^2 + \ddot{I}_{yy}^2 - \frac{1}{3} \ddot{I}^2 \right)
\end{aligned}$$

By substituting the quadrupole moment values we get

$$\frac{dE}{dt} = -\frac{8G^4}{15c^5} \frac{m_1^2 m_2^2}{(1-e^2)^2} [12(1+e \cos \theta)^2 + e^2 \sin^2 \theta] \dot{\theta}^2$$

this is the instantaneous loss due to radiation. Let $k = -\frac{8G^4}{15c^5} \frac{m_1^2 m_2^2}{(1-e^2)^2}$, therefore

$$\frac{dE}{dt} = k [12(1+e \cos \theta)^2 + e^2 \sin^2 \theta] \dot{\theta}^2 \quad (4.38)$$

The period of the binary is given by,

$$T = \int_0^{2\pi} \frac{1}{\dot{\theta}} d\theta \quad (4.39)$$

we have

$$\dot{\theta} = \frac{[(m_1 + m_2)a(1-e^2)]^{\frac{1}{2}}}{r^2} = \frac{c_2}{r^2}$$

where $c_2 = [(m_1 + m_2)a(1-e^2)]^{\frac{1}{2}}$. Substituting in Eq.(4.39) we get

$$\begin{aligned}
T &= \int_0^{2\pi} \frac{r^2}{c_2} d\theta \\
T &= \frac{c_1}{c_2} \int_0^{2\pi} \frac{1}{(1+e \cos \theta)^2} d\theta
\end{aligned}$$

Solving for the integral, we get

$$T = \frac{2\pi c_1}{(1-e^2)^{\frac{3}{2}}}$$

substituting the values of the constants

$$\begin{aligned}
T &= \frac{a^2 (1-e^2)^2}{\sqrt{(m_1 + m_2) a (1-e^2)}} \times \frac{2\pi}{(1-e^2)^{\frac{3}{2}}} \\
T &= \sqrt{\frac{2\pi a^3}{(m_1 + m_2)}}
\end{aligned}$$

The average value of the power radiated over the orbital period is given by

$$\left\langle \frac{dE}{dt} \right\rangle = \frac{1}{T} \int_0^T \frac{dE}{dt} dt$$

We can write it as

$$\left\langle \frac{dE}{dt} \right\rangle = \frac{1}{T} \int_0^T \frac{dE}{dt} \frac{1}{\dot{\theta}} d\theta$$

substituting for $\frac{dE}{dt}$ from Eq.(4.38), we get

$$\left\langle \frac{dE}{dt} \right\rangle = \frac{1}{T} \int_0^T k [12(1 + e \cos \theta)^2 + e^2 \sin^2 \theta] \dot{\theta} d\theta$$

substituting for $\dot{\theta}$ and r ,

$$\begin{aligned} \left\langle \frac{dE}{dt} \right\rangle &= \frac{kc_2}{Tc_1} \int_0^{2\pi} [12(1 + e \cos \theta)^2 + e^2 \sin^2 \theta] (1 + e \cos \theta)^2 d\theta \\ \left\langle \frac{dE}{dt} \right\rangle &= \frac{kc_2}{Tc_1} \left\{ \int_0^{2\pi} 12(1 + e \cos \theta)^4 d\theta + \int_0^{2\pi} e^2 \sin^2 \theta (1 + e \cos \theta)^2 d\theta \right\} \end{aligned}$$

solving the integrals,

$$\left\langle \frac{dE}{dt} \right\rangle = \frac{kc_2}{Tc_1} \left\{ 24 + 9e^2 (8 + e^2) + e^2 + \frac{e^4}{4} \right\} \pi$$

substituting for the constants c_1, c_2, T and k

$$\begin{aligned} \left\langle \frac{dE}{dt} \right\rangle &= -\frac{4G^4}{15c^5} \frac{m_1^2 m_2^2 (m_1 + m_2)}{a^5 (1 - e^2)^{\frac{7}{2}}} \left\{ 24 + 73e^2 + \frac{37}{4}e^4 \right\} \\ \left\langle \frac{dE}{dt} \right\rangle &= -\frac{32G^4}{5c^5} \frac{m_1^2 m_2^2 (m_1 + m_2)}{a^5 (1 - e^2)^{\frac{7}{2}}} \left(1 + \frac{73}{24}e^2 + \frac{37}{96}e^4 \right) \end{aligned} \quad (4.40)$$

Loss of angular momentum

From Eq.(3.18) we have

$$\begin{aligned} \frac{dL}{dt} &= -\frac{2}{5} \epsilon^{z\alpha\beta} \ddot{Q}_\alpha^\gamma \ddot{Q}_{\gamma\beta} \\ &= -\frac{2}{5} \epsilon^{z\alpha\beta} \ddot{I}_\alpha^\gamma \ddot{I}_{\gamma\beta} \\ \frac{dL}{dt} &= -\frac{2}{5} \left[\ddot{I}_{xy} (\ddot{I}_{yy} - \ddot{I}_{xx}) + \ddot{I}_{xy} (\ddot{I}_{xx} - \ddot{I}_{yy}) \right] \end{aligned}$$

substituting the values, we get

$$\frac{dL}{dt} = -\frac{8}{5} \frac{m_1^2 m_2^2}{a^2 (1 - e^2)^2} [4 + 10e \cos \theta + e^2 (9 \cos^2 \theta - 1) + e^3 (3 \cos^3 \theta - \cos \theta)] \dot{\theta}$$

simplifying we have

$$\frac{dL}{dt} = c_3 [4 + 10e \cos \theta + e^2 (9 \cos^2 \theta - 1) + e^3 (3 \cos^3 \theta - \cos \theta)] \dot{\theta} \quad (4.41)$$

The average of angular momentum over the period is defined as

$$\left\langle \frac{dL}{dt} \right\rangle = \frac{1}{T} \int_0^T \frac{dL}{dt} dt$$

From Eq.(4.39) substituting for $\frac{dL}{dt}$,

$$\left\langle \frac{dL}{dt} \right\rangle = \frac{1}{T} \int_0^{2\pi} \frac{dL}{dt} \frac{d\theta}{\dot{\theta}}$$

$$\left\langle \frac{dL}{dt} \right\rangle = \frac{c_3}{T} \int_0^{2\pi} [4 + 10e \cos \theta + e^2 (9 \cos^2 \theta - 1) + e^3 (3 \cos^3 \theta - \cos \theta)] d\theta$$

Solving for the integral, we get

$$\left\langle \frac{dL}{dt} \right\rangle = \frac{c_3}{T} \{8\pi + 9\pi e^2 + -2\pi e^2\}$$

substituting the values of c_3 and T we get,

$$\left\langle \frac{dL}{dt} \right\rangle = -\frac{32}{5} \frac{m_1^2 m_2^2 (m_1 + m_2)^{\frac{1}{2}}}{a^{\frac{7}{2}} (1 - e^2)^2} \left(1 + \frac{7}{8} e^2\right) \quad (4.42)$$

Change in orbital parameters of binary

Now we can determine how the orbital parameters changes due to the loss of energy and angular momentum from the system. The average value of the change in periastron position of the binary system is given by,

$$\left\langle \frac{da}{dt} \right\rangle = \frac{2a^2}{m_1 m_2} \left\langle \frac{dE}{dt} \right\rangle$$

Substituting the average value of the energy lost from Eq.(4.40) we get,

$$\left\langle \frac{da}{dt} \right\rangle = -\frac{64}{5} \frac{m_1 m_2 (m_1 + m_2)}{a^3 (1 - e^2)^{\frac{7}{2}}} \left(1 + \frac{73}{24} e^2 + \frac{37}{96} e^4\right) \quad (4.43)$$

The average value of the rate of change of eccentricity is ,

$$\left\langle \frac{de}{dt} \right\rangle = \frac{(m_1 + m_2)}{m_1 m_2 e} \left[\frac{a (1 - e^2)}{(m_1 + m_2)} \left\langle \frac{dE}{dt} \right\rangle - \frac{(1 - e^2)^{\frac{1}{2}}}{a^{\frac{1}{2}} (m_1 + m_2)^{\frac{1}{2}}} \left\langle \frac{dL}{dt} \right\rangle \right] \quad (4.44)$$

substituting the values from Eqns.(4.40) & (4.42),

$$\left\langle \frac{de}{dt} \right\rangle = -\frac{304}{15} \frac{m_1 m_2 (m_1 + m_2) e}{a^4 (1 - e^2)^{\frac{5}{2}}} \left(1 + \frac{121}{304} e^2\right) \quad (4.45)$$

We consider binary systems consisting of pulsars and obtain the change in orbital parameters using the results obtained in this section.

Table 4.1: Binary pulsar systems

Pulsar Name	Pulsar mass (M_\odot)	Companion mass (M_\odot)	Eccentricity	Semi-major axis (km)
B1913+16	1.441	1.387	0.617134	1.95×10^6
J1518+4904	1.56	1.05	0.24948451	17×10^6
B1534+12	1.3332	1.3452	0.27367752	2.283×10^6
B2127+11C	1.349	1.363	0.681395	1.97×10^6
J0737-3039	1.338	1.242	0.08778	0.9×10^6

Table 4.2: Calculated parameters

Pulsar Name	$\langle \frac{da}{dt} \rangle (km/yr)$	$\langle \frac{de}{dt} \rangle (yr^{-1})$	$\langle \frac{dL}{dt} \rangle (M_\odot km^2/yr^2)$	$\langle \frac{dE}{dt} \rangle (M_\odot km^2/yr^3)$
B1913+16	-3.52608	-5.68898×10^{-10}	-5.05764×10^6	-1.2235×10^{11}
J1518+4904	-5.06301×10^{-4}	-9.49403×10^{-15}	-575.212	-189456
B1534+12	-0.254453	-3.74094×10^{-11}	-817316	-5.78097×10^9
B2127+11C	-5.64381	-7.86174×10^{-10}	-5.69969×10^6	-1.76535×10^{11}
J0737-3039	-2.41308	-3.62408×10^{-10}	-1.47013×10^7	-3.26851×10^{11}

Massive binaries emit more gravitational waves than less massive ones. The change in orbital separation and eccentricity is more for massive systems.

Chapter 5

Newtonian chirp from inspiraling binaries

We study the gravitational waves produced from circular binaries in leading order (quadrupole) using the expressions derived in last chapter. In general, the orbits of the two bodies are approximately ellipses, but it has been shown that long before the coalescence of the two bodies, the orbits become circular atleast for long-lived binaries due to gravitational radiation.

5.1 Newtonian Chirp

Gravitational waves are the reasons for perturbations in space-time. For a circular binary using Einstein's quadrupole formula we have already obtained the strain/perturbation to be

$$h(t) = A(t)\cos(\phi) \quad (5.1)$$

where $A(t)$ is the amplitude and $\phi(t)$ is the gravitational wave phase.

$$A(t) = \frac{4\mathcal{M}^{5/3}\pi^{2/3}F(t)^{2/3}}{D} \quad (5.2)$$

$$\phi(t) = \phi_0 - 2 \left[\frac{1}{256(\pi f_0 \mathcal{M})^{8/3}} - \frac{t}{5\mathcal{M}} \right]^{5/8} \quad (5.3)$$

$F(t)$ is the instantaneous wave frequency and f_0 is the initial frequency of the wave and the constant ϕ_0 is the GW phase when the signal is received in detectors at $t = 0$. We have the merging time given by the expression

$$\tau_m = \frac{5}{256(\pi f_0)^{8/3}\mathcal{M}^{5/3}} \quad (5.4)$$

$$F(t) = f_0 \left(1 - \frac{t}{\tau_m} \right)^{-3/8} \quad (5.5)$$

Starting from an initial frequency at $t = 0$, the frequency and amplitude of gravitational wave increases with time. Hence the gravitational wave signal is called as chirp. The above equations governing the gravitational waves are based on leading order contribution from quadrupole mo-

ment of the system obtained using linearized gravity. In literature there exists post-Newtonian approximation formalism where gravitational wave strain, binary frequency and gravitational wave phase is expressed in form of series of terms where each term contributes [12]. If the leading order contribution alone is taken ignoring the subsequent terms in post-Newtonian approximation then we obtain the same expressions [9, 10], and the gravitational wave signal is called as Newtonian chirp [9, 10].

The instantaneous frequency of gravitational wave is twice the instantaneous frequency of the binary system from which it is produced. The separation between the masses is governed by the equation

$$a = a_0 \left(1 - \frac{t}{\tau_m}\right)^{1/4} \quad (5.6)$$

Where at $t = \tau_m$ the separation between the masses becomes zero. This is the merging time at which the corresponding binary frequency $\omega^2 = M/a^3$ goes to ∞ , thus we can see that at this instant the frequency of gravitational waves also shoots to ∞ .

The singular value of frequency is due to the merging of two point masses in which inspiral continues till $a = 0$. However, in general relativity it is seen that not all the orbits are stable till $a = 0$ and the inner most stable circular orbit (ISCO) corresponds to $a = 6M_\odot$ [11]. Hence in post-Newtonian approximation, the inspiral phase is taken to end at this orbital separation, where the stars begin to interact and merge. The corresponding gravitational wave frequency at this separation is given by

$$F_{ISCO} \approx \frac{4400}{M} Hz \quad (5.7)$$

Inspirational phase is followed by a short lived-merger phase. The merger phase begins when the masses starts to merge into a single object. After this the ring-down phase starts where the new object formed radiates away the deformations resulted from merging [12]. Gravitational waves are produced in all these phases. The merger phase is studied by solving Einstein's equation numerically whereas perturbation theory is required for ring-down phase.

Gravitational waves are continuously produced by binary systems and many of them might reach earth but can be too weak to be noticed in the LASER interferometer detectors. As the inspiral phase of the binary system continues, the frequency of orbital motion increases and if it reaches a value at which the signal is strong enough to be detected, we start seeing the GW from this frequency value (called as initial frequency). Ground based gravitational wave detectors are capable of detecting signals of frequency greater than 10 Hz. At lower frequencies the sources from space is overcome by seismic and other earth-based environmental noise sources [11]. Hence in this study we are interested in the beginning of signal in the detector at $t = 0$ starting at $f_0 = 10\text{Hz}$.

5.2 Binaries at galactic center

We reside in the milky way galaxy. The galactic center is located at 8 Kpc distance from Earth. We consider Black Hole-Black Hole (BH-BH) binary, Black Hole-Neutron Star (BH-NS) binary,

Black Hole-White dwarf (BH-WD) binary, Neutron Star-Neutron Star (NS-NS) binary, Neutron Star-White dwarf (NS-WD) binary and White dwarf-White dwarf (WD-WD) binary being at our galactic center. Chandrasekhar's limit gives the maximum mass of a stable white dwarf star which is about $1.39M_{\odot}$. Most white dwarf stars are less massive than this value, so we have taken the mass of white dwarf star for Newtonian chirp study to be $1M_{\odot}$. The theoretical value of maximum mass of a stable neutron star is uncertain [13]. Tolman-Oppenheimer-Volkoff (TOV) limit gives the maximum mass of stable neutron star, the modern estimates range from approximately $1.5M_{\odot}$ - $3M_{\odot}$. Equation of state for extremely dense matter is not well known and hence there exists an uncertainty in the limit. The observational data suggests that mass of most of the pulsars lies between $1.30M_{\odot}$ to $1.50M_{\odot}$ [13]. With this regard we take the mass of neutron star to be $1.4M_{\odot}$ in this study. Since there exists no well defined limit on mass of neutron star for gravitational collapse we consider the black hole to be of $10M_{\odot}$.

We assume that at time $t = 0$ the frequency of gravitational wave received in detector to be $f_0 = 10$ Hz. We can find the orbital frequency of the masses in the binary system, $f_{system} = f_0/2 = 5$ Hz. Gravitational waves takes time to travel from binaries to earth. On receiving in detector at $t = 0$ if the gravitational wave has initial frequency of 10 Hz it doesn't imply that the binaries are currently orbiting at 5 Hz, but it should be thought of as the information encoded about binary system in gravitational waves signal at $t = 0$. The aim is to see for a binary system undergoing 5 orbital rotation per second whose corresponding gravitational wave signal arrives with frequency 10 Hz on Earth, what will be the waveform and frequency variation as they inspiral to merge. We use the binary parameters: masses of two stars, distance from the earth and frequency of orbiting in the Mathematica code to obtain the plots in figure [5.1], [5.2], & [5.3].

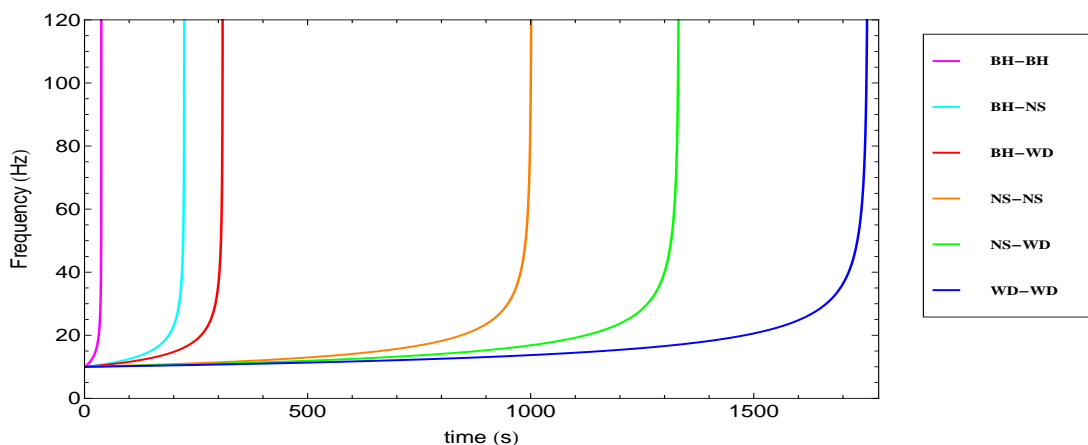


Figure 5.1: Frequency variation plot of compact binaries

It can be seen that the waveforms produced from Mathematica code starts at $t = 0$ and extends till the merging time τ_m which can be calculated from the formula. The frequency varies from the initial value starting at $t = 0$ and approaches to infinity at τ_m .

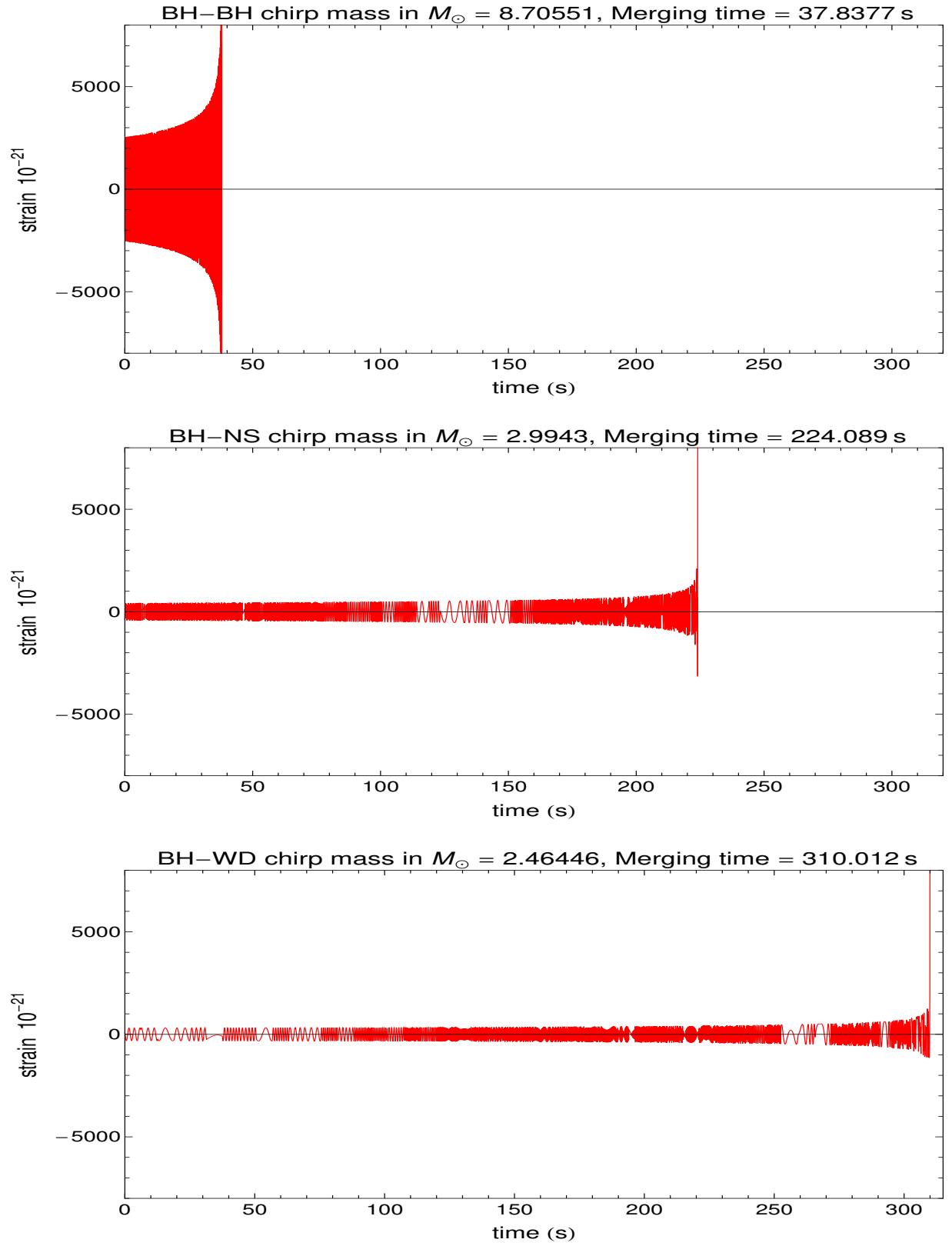


Figure 5.2: Newtonian chirp of BH-BH,BH-NS,BH-WD

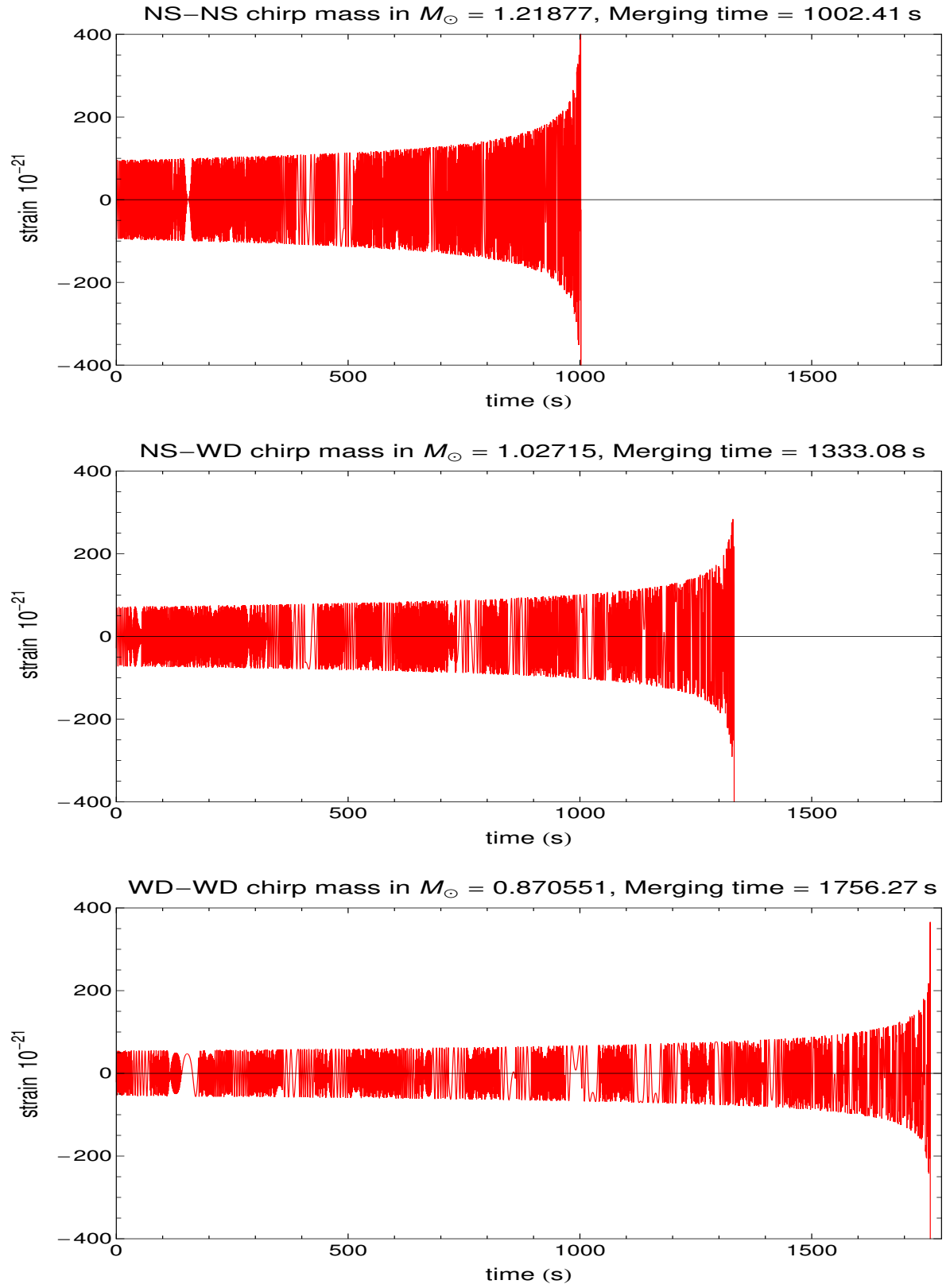


Figure 5.3: Newtonian chirp of NS-NS, NS-WD, WD-WD

Table 5.1: Compact binaries at galactic center

Compact binary	Masses(M_\odot)			Peak strain(approx)	Merging time	Peak freq.
	m_1	m_2	\mathcal{M}	h_{peak}	τ_m (sec)	F_{ISCO} (Hz)
BH-BH	10	10	8.7005	8000×10^{-21}	37.8377	220
BH-NS	10	1.4	2.9943	2000×10^{-21}	224.089	385.96
BH-WD	10	1	2.46446	1000×10^{-21}	310.012	400
NS-NS	1.4	1.4	1.2187	400×10^{-21}	1002.41	1571.43
NS-WD	1.4	1	1.02715	250×10^{-21}	1333.08	1833.33
WD-WD	1	1	0.870551	200×10^{-21}	1756.27	2200

For binaries at same distance from Earth with same initial orbital frequency in terms of merging time τ_m we can arrange as-

$$\tau_m(BH - BH) < \tau_m(BH - NS) < \tau_m(BH - WD) < \tau_m(NS - NS) < \tau_m(NS - WD) < \tau_m(WD - WD)$$

For binaries at same distance from Earth with same initial orbital frequency in terms of peak strain S_p we can arrange as-

$$S_p(BH - BH) > S_p(BH - NS) > S_p(BH - WD) > S_p(NS - NS) > S_p(NS - WD) > S_p(WD - WD)$$

With point mass consideration in terms of variation of frequency per unit time (δV_f) in 10 Hz to 40 Hz interval we can arrange as-

$$\delta V_f(BH - BH) > \delta V_f(BH - NS) > \delta V_f(BH - WD) > \delta V_f(NS - NS) > \delta V_f(NS - WD) > \delta V_f(WD - WD)$$

Massive binaries lose large amount of energy in the form of gravitational waves hence they inspiral more rapidly which can very well be seen in their frequency-time plot. They rapidly sweep through frequency interval 10Hz–40Hz compared to less massive binaries. They also undergo less number of cycles due to rapid inspiral which can be seen in their waveforms and they merge faster. In case of less massive binaries, since they emit small amount of gravitational they inspiral slowly, they sweep through frequency interval 10 Hz–40 Hz slowly undergoing large number of cycles and take comparatively longer time to merge. Since massive binaries emit more gravitational radiation during their inspiral phase than less massive ones their magnitude of strain is always more during the evolution stage and at the end of inspiral stage they attain peak strain larger than less massive ones.

Different binary systems end up their inspiral phase with final orbital frequency given by $F_{ISCO}/2$, which depends inversely upon the total mass of system. This is based upon the assumption that masses are treated as point objects hence in reality the binaries may end up with different orbital frequency before merging, as their size and radius may cause them to collide and merge prior to reaching peak frequency.

5.3 Supermassive black holes and slowly orbiting systems

Supermassive black holes can have masses ranging from few hundred solar masses to thousands of solar mass. We have considered a supermassive BH-BH binary with each BH having a mass

of $100M_{\odot}$ and another such system with each BH having a mass of $200M_{\odot}$. The binaries are taken to be located outside our galaxy at 500 Mpc orbiting at 5 Hz. We have obtained its waveform and the frequency variation plot in figure [5.4] and the results tabulated in table [5.2].

For supermassive black hole binaries with masses $100M_{\odot}$ each and $200M_{\odot}$ each, orbiting at 5 Hz the merging happens within a second and their F_{ISCO} values being 22 Hz and 11 Hz respectively lies very near to gravitational wave starting frequency 10 Hz. The study of these supermassive black holes reveal that by the time 5Hz is reached in their evolution stage which makes their gravitational signal cross the seismic noise frequency 10 Hz and detectable in ground based interferometer detectors they are at very end of their inspiral stage and merge within a second, hence rather than inspiral phase the merger and ring-down phases are more possible to be detected in aLIGO .

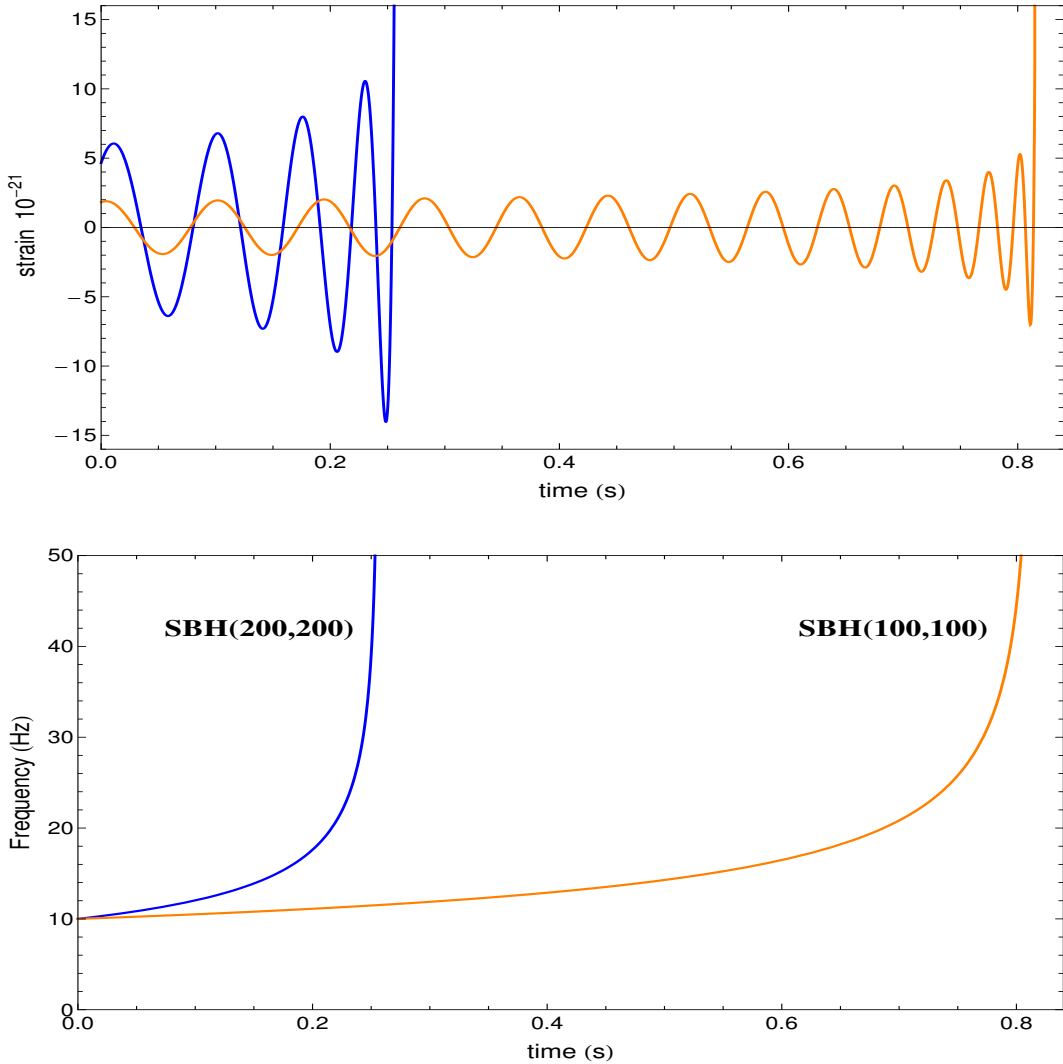


Figure 5.4: Newtonian chirp and frequency variation plots of supermassive blackholes observed from 500 Mpc

For supermassive black hole binary with mass $1000M_{\odot}$ the F_{ISCO} comes out to be 4.4 Hz and for 10^6M_{\odot} the F_{ISCO} comes out to be 4.4×10^{-3} , hence their gravitational waves in inspiral phase never reach 10 Hz to be observed in aLIGO. Considerable inspiral phase

of GW from these supermassive black holes can be seen using Laser Interferometer Space Antenna(LISA) which has observable frequency in milli-hertz [14]. The astrophysical process where merging of supermassive black holes can be seen is in merging of two galaxies. There exists observational evidence that every galaxy has a supermassive black hole at its center and hence the supermassive BH-BH merger is very likely to happen. Strong evidence of supermassive black hole binary exist in NGC 6240 , it is considered as a new galaxy formed by the merging of two different galaxies. The two black holes present in it are currently about 3000 light-years apart. The galaxy spans only 300000 light-years so it is expected that the black holes will merge to form a single black hole.

Table 5.2: SBH binary at 500 Mpc

Masses(M_{\odot})			strain	τ_m	F_{ISCO}
m_1	m_2	\mathcal{M}	h_{peak}	(sec)	(Hz)
100	100	87.0051	10^{-21}	0.815188	22
200	200	174.11	10^{-21}	0.256768	11

Not all binary systems orbit very rapidly to have a orbital frequency of 5 Hz, so we consider slowly orbiting binaries for our discussion. The orbital frequency of known double neutron star systems comes out to be about 10^{-6} Hz so we assume that initially the double neutron star system possesses this frequency. We also consider WD-WD binary orbiting at the same frequency. Hence, the arriving gravitational waves is seen with initial frequency of 2×10^{-6} Hz. We assume both the systems to be located at 1pc distance. The waveform and frequency variation plot can be obtained for these systems, the results are tabulated in table [5.3].

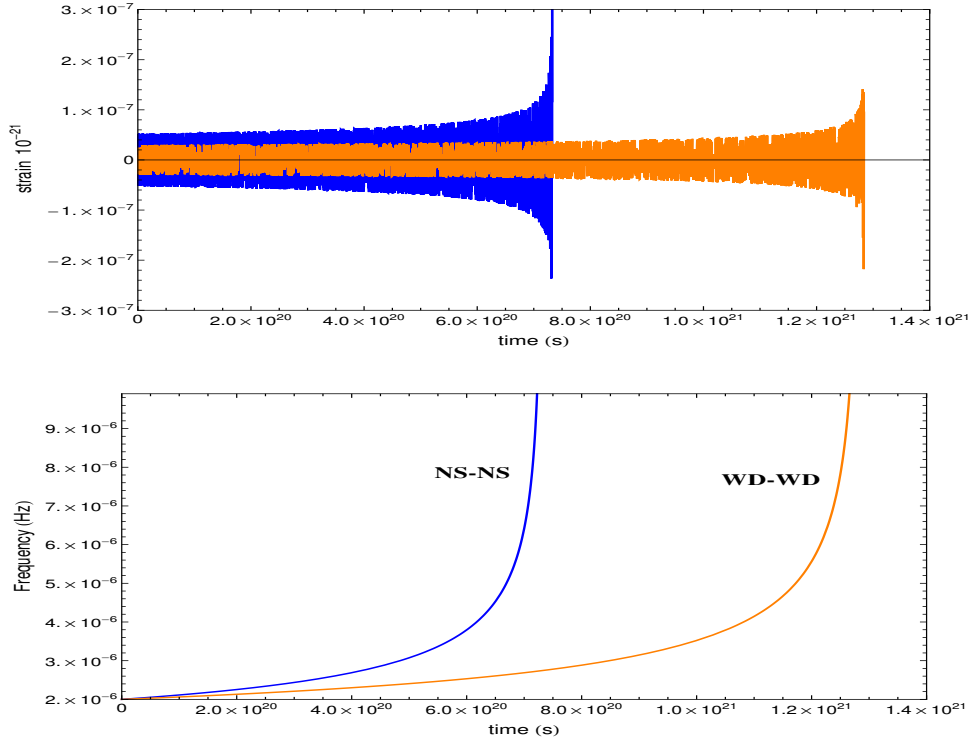


Figure 5.5: Slowly orbiting systems

Table 5.3: Slowly orbiting binary system at 1 pc

System	Masses(M_\odot)			Peak strain order	Merging time	Peak freq.
	m_1	m_2	\mathcal{M}	h_{peak}	τ_m (sec)	F_{ISCO} (Hz)
NS- NS	1.4	1.4	1.21877	10^{-21}	7.32765×10^{20}	1571.43
WD-WD	1	1	0.870551	10^{-21}	1.28384×10^{21}	2200

The merging time of slowly orbiting NS-NS system comes out to be 7.32765×10^{20} sec and WD-WD system comes out to be 1.28384×10^{21} sec whereas the age of our universe is 13.799×10^9 yrs = 4.35165×10^{17} sec. Hence compact binary systems which at present are slowly orbiting their merger is not likely to be seen in aLIGO anytime in future. The detections of NS-NS merger, NS-WD merger and WD-WD merger if is spotted in aLIGO then those systems must have evolved in cosmic times to reach this late inspiral stage or they had a very less orbital separation and relatively large orbital frequency at the time of formation or due to any other factor.

5.4 GW150914

LIGO collaboration discovered gravitational waves produced from merging event. The events detected by LIGO are named as GW followed by date in YYMMDD format.

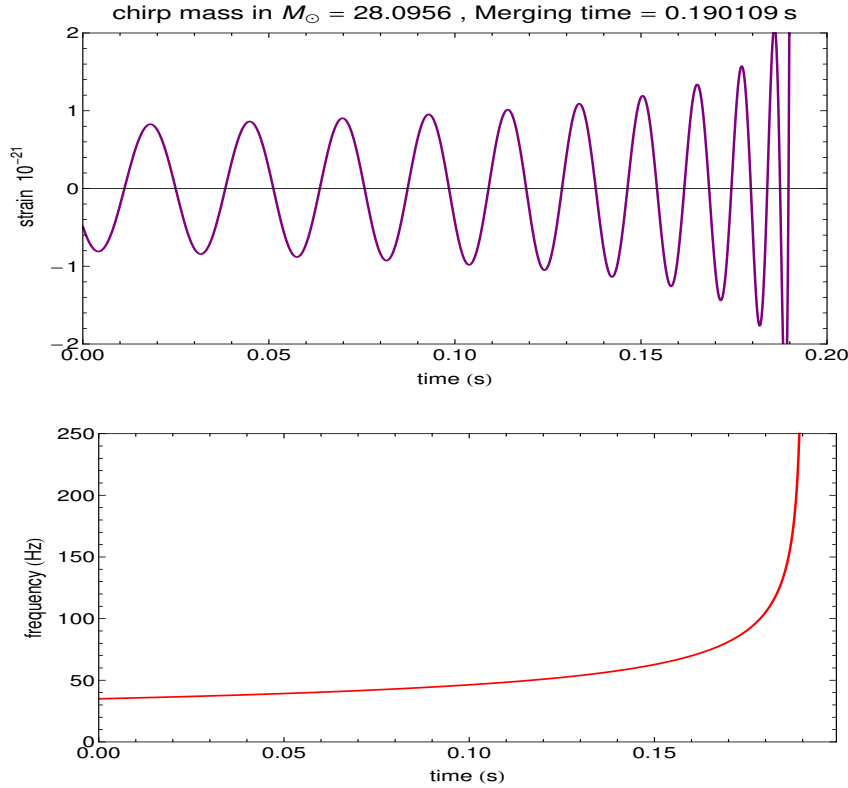


Figure 5.6: LIGO events Newtonian chirp

When GW150914 was received in detectors it had a strain which attained peak order of 10^{-21} , this signal was seen to increase in frequency from 35Hz and reached 250 Hz in about

0.2 seconds. It was seen that in 8 cycles the signal increased from 35 Hz to 150 Hz [15]. The gravitational wave frequency of 150 Hz corresponds to the orbital frequency of 75 Hz for the binary system. For Newtonian point mass binary this gives 350 Km as the orbital separation. The WD-WD, NS-NS or NS-BH merger should occur at a much larger distance than this value hence LIGO collaboration suggested that the signal to be from a BH-BH binary. This was the first direct observation of black holes and their existence. The masses of binary system could be computed from data analysis and estimated to be $36M_{\odot}$ and $29M_{\odot}$ [15]. The luminous distance of this system was estimated to be 410 Mpc. We take the parameters of GW150914 to obtain the Newtonian Chirp plot in figure [5.6]. The strain recorded by LIGO's Livingston detector for GW150914 is plotted along with the inspiral part from Newtonian chirp with F_{ISCO} as inspiral limit in figure[5.7]. The F_{ISCO} comes out to be 67.69 Hz and the time corresponding to it can be found from frequency-time plot of Newtonian chirp. For a signal starting at 0.25 seconds this corresponds to 0.407 seconds. The Newtonian chirp doesn't mimic exactly the real signal's amplitude and phase observed, but its worth appreciating that the strain order and evolution during inspiral phase has resemblance. This is to be expected as higher order terms of Post-Newtonian approximation if considered bring changes in phase and amplitude. We can also see that merger and ring-down part of the actual signal is not captured by the Newtonian chirp.

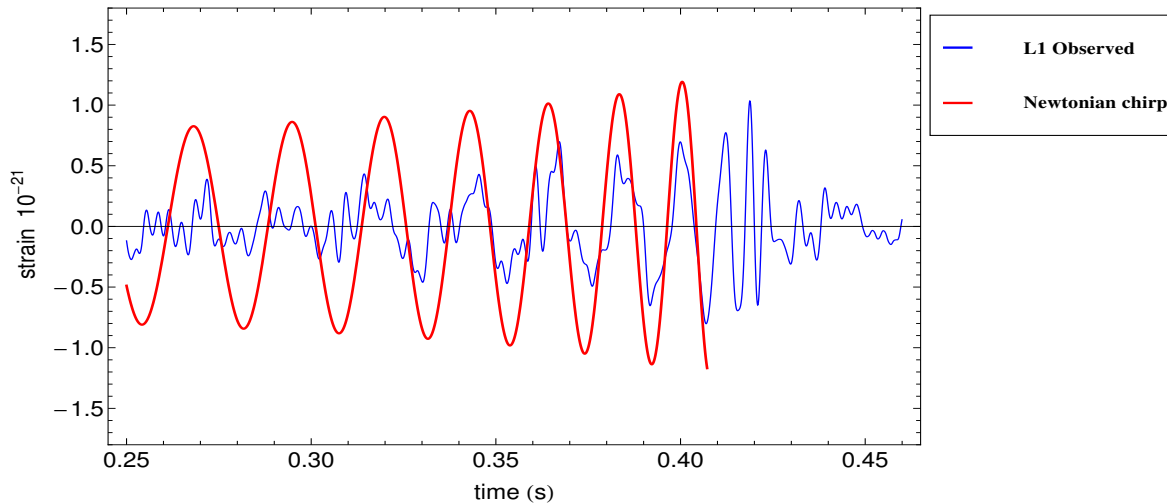


Figure 5.7: GW150914 Livingston observed with Newtonian chirp

5.5 Amplitude spectral density

Theoretically the possible sources and distances of them which can be observed can be found using thing the amplitude spectral density of sources and sensitivity curves of detectors. The power spectral density S_h is the power per unit frequency. The square root of the power spectral density gives the amplitude spectral density defined as $h_f = \sqrt{S_h}$. If h_f of the source lies above the sensitivity curve of the detector then the source can be detected. For a source the amplitude spectral density is given by ,

$$\sqrt{S_h} = h_c f^{-1/2} = 2f^{1/2} |\tilde{h}_c| \quad (5.8)$$

where h_c is characteristic strain and \tilde{h}_c is the Fourier transform of signal. For inspiraling binaries in the leading order it has been found that,

$$\tilde{h}_c = A(f)e^{i\psi}$$

where

$$A(f) = \sqrt{\frac{5}{24}} \frac{\mathcal{M}^{5/6}}{D\pi^{2/3}} f^{-7/6} \quad (5.9)$$

$$\psi = 2\pi f t_0 - \phi_0 - \pi/4 + \frac{3}{128} (\pi \mathcal{M} f)^{-5/3}$$

Using the above expressions we get,

$$\sqrt{S_h} = 2f^{1/2} |\tilde{h}_c| = \sqrt{\frac{5}{6}} \frac{\mathcal{M}^{5/6}}{D\pi^{2/3}} f^{-2/3} \quad (5.10)$$

In inspiral a gravitational wave signal spends greater number of cycles in lower frequency whereas lesser number of cycles in higher frequency. Since the amplitude spectral density h_f is inversely related to frequency, with increase in frequency h_f decreases. Detectors sensitivity curve is governed by various noises present in the detector. We plot the h_f vs frequency plot for the various chosen compact binaries and also for the GW150914 along with the LIGO design sensitivity curve and aLIGO design sensitivity curve to see if the signal could be detected. The area between the signal curve and detector's noise curve indicates the signal to noise ratio.

We first consider the compact binaries in their location at galactic center and then at 410 Mega parsec (the distance from which GW150914 originated). We keep the distance of GW150914 event its respective one to obtain the plots shown in figures [5.8] & [5.9].

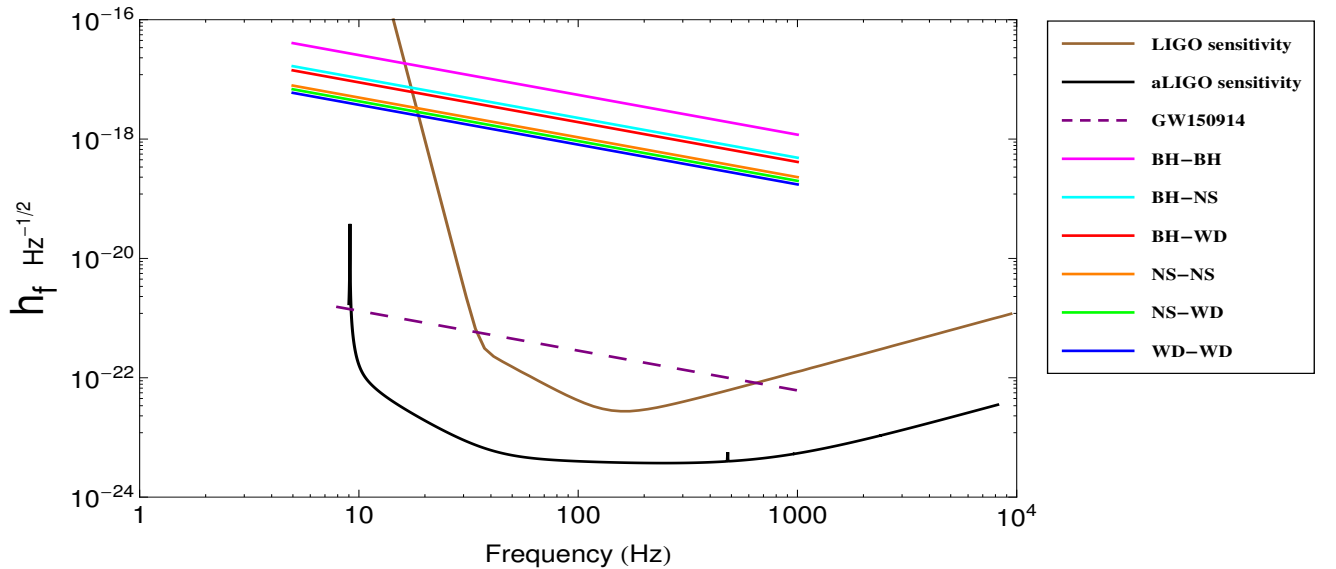


Figure 5.8: Compact binaries at 8 Kpc along with GW150914

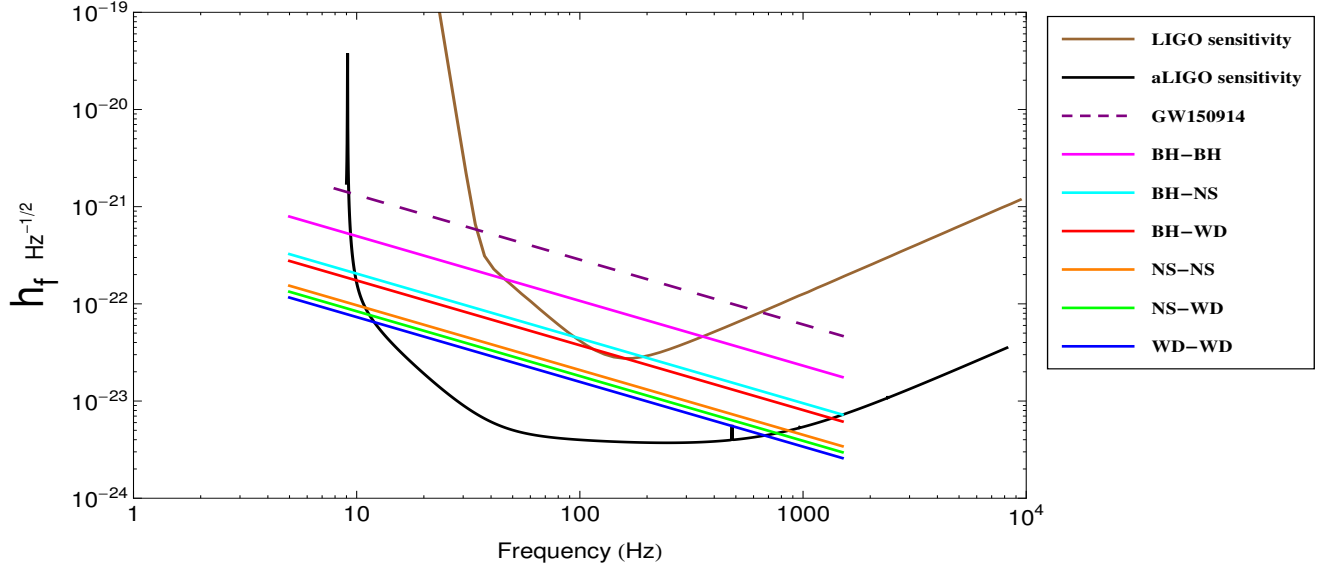


Figure 5.9: Compact binaries at 410 Kpc along with GW150914

In the plot with Newtonian chirp context we have extended the frequency of these systems till 1000 Hz but the inspiral phase of each compact binary will end at their respective peak frequency F_{ISCO} . The amplitude spectral density during merger and ring-down phases shows different dependence on frequency than inspiral phase.

The amplitude spectral density curve of compact binaries at galactic center (8kpc) lie above LIGO and aLIGO sensitivity curve, hence they are within the detector detection capabilities. When the same binaries are located at 410 Mpc only the BH-BH is well within the detection capability of LIGO whereas BH-NS and BH-WD systems lie very slightly above the LIGO curve in a small frequency range but extracting the signal from noise is hard. The NS-NS, NS-WD and WD-WD systems lie below the sensitivity curve of LIGO at all frequency values. Even when located at 410 Mpc NS-NS, NS-WD and WD-WD systems are in detection capabilities of aLIGO. Hence the merger of these systems can be expected to be observed in future. GW150914 signal lies well above the aLIGO detector sensitivity whereas the NS-NS, NS-WD and WD-WD binary curve located at 410 Mpc lies over the aLIGO curve lowest among the all. Hence sophisticated data analysis is required to pull out such signals from noise.

5.6 Data analysis from waveform

Gravitational waves are produced from binaries during inspiral phase, merger phase, and ring-down phase. The chirp mass is always determined using inspiral phase. Though the actual gravitational wave analysis involves sophisticated methods, the essential use of Newtonian chirp formulas in interpreting the gravitational wave signal is described in this section. We discuss regarding how to look at the gravitational waveform and find the parameters of gravitational waves and binary system. Let us suppose that a signal was received detector is as in figure [5.10] (It is a waveform obtained using Newtonian chirp in Mathematica code).

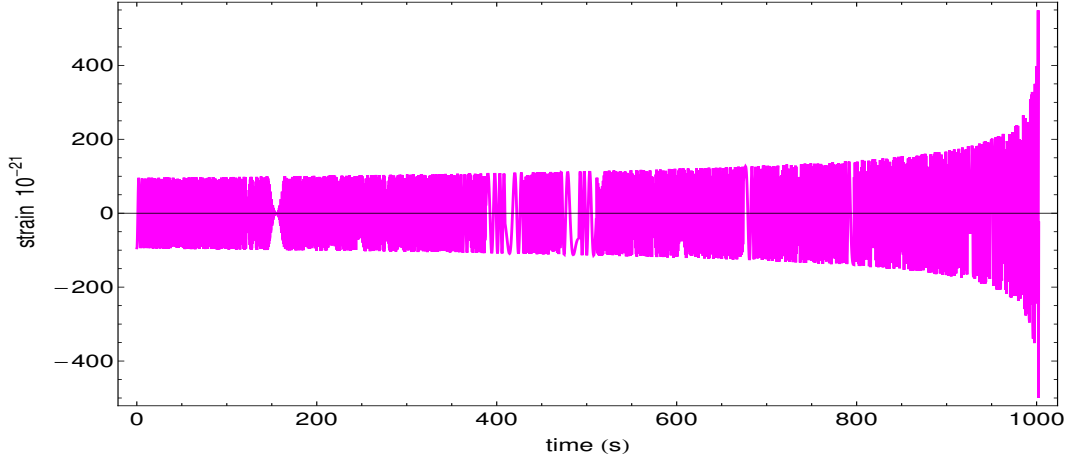


Figure 5.10: Gravitational waveform for analysis

It is always easy to find the initial frequency (the frequency of the wave received by detector at $t = 0$), by calculating the number of waves during the first second of receiving the waves gives its frequency.

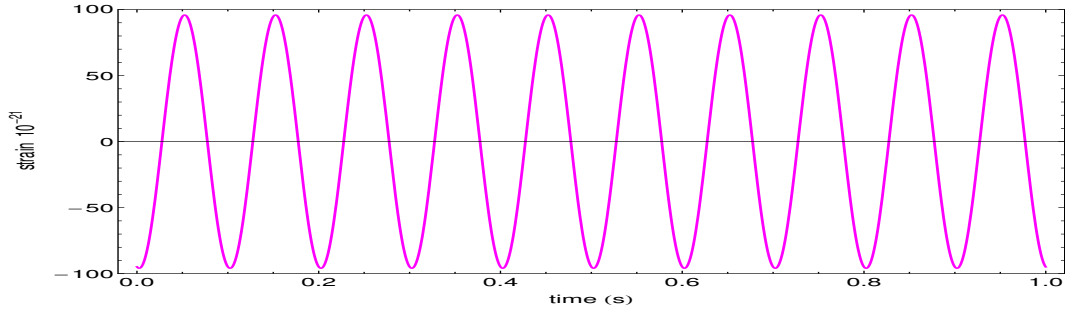


Figure 5.11: waveform observed during the first second of arrival

It is seen that during the time interval of $t = 0$ to $t = 1$ sec the signal has 10 full cycles, hence the initial frequency is 10 Hz. Next we consider the waveform detected during $t = 500$ sec and $t = 501$ sec.

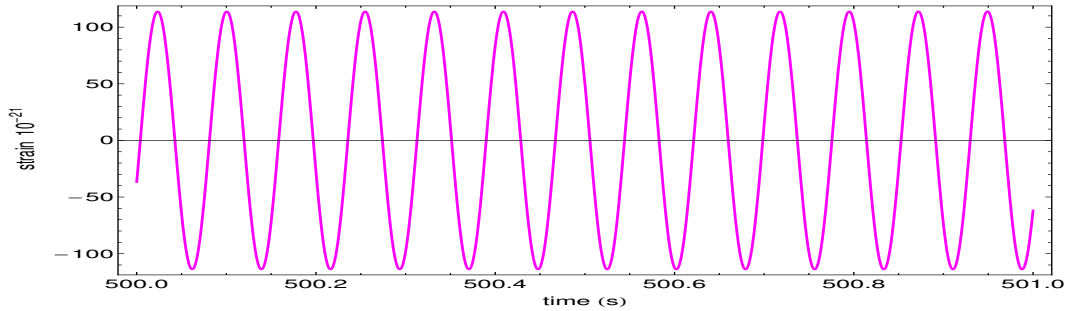


Figure 5.12: waveform observed from 500 – 501s with frequency $\simeq 13\text{Hz}$

The waveform in this interval has approximately 13 full cycles. This implies frequency at $t = 500$ sec is about 13Hz. We have the initial frequency $f_0 = 10$ Hz and the instantaneous frequency value 13 Hz at $t = 500$ sec. With this we can find chirp mass \mathcal{M} using the instantaneous

frequency formula:

$$F(t) = f_0 \left(1 - \frac{t}{\tau_m} \right)^{-3/8}$$

substituting the value of τ_m from Eq.(5.4), we have

$$F(t) = f_0 \left(1 - \frac{t}{\frac{5}{256(\pi f_0)^{8/3} \mathcal{M}^{5/3}}} \right)^{-3/8} \quad (5.11)$$

the value of chirp mass can be determined using the formula,

$$\mathcal{M} = \left\{ \left[1 - (f/f_0)^{(-8/3)} \right] 5 \left(256t(\pi f_0)^{(8/3)} \right)^{-1} \right\}^{-3/5} (4.92549095 * 10^{-6})^{-1} \quad (5.12)$$

Substituting the values of $f_0 = 10$ Hz, $f = 13$ Hz, $t = 500$ sec, we get $\mathcal{M} = 1.22526 M_\odot$. For a much better value of chirp mass we can consider waveform detected during the time interval $t = 900$ sec and $t = 901$ sec.

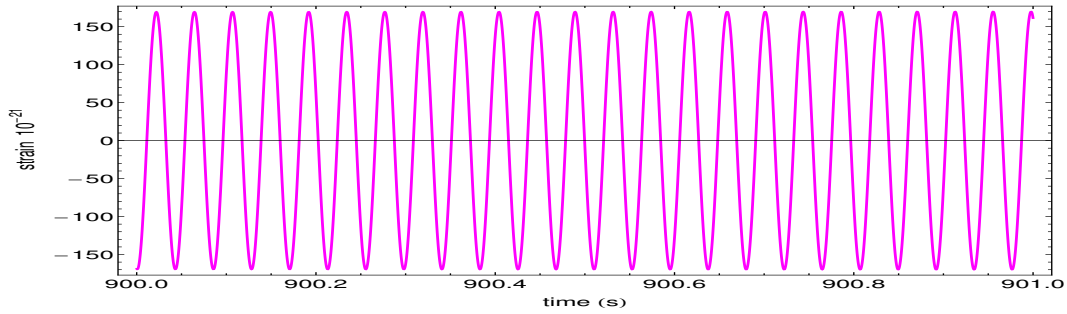


Figure 5.13: waveform observed from 900- 901s with frequency $\simeq 24$ Hz

The frequency of the wave is about 23 Hz, by using initial frequency value we can evaluate the chirp mass using $f = 24$ Hz and $t = 900$ sec we get $\mathcal{M} = 1.22309 M_\odot$. The average of two values of chirp mass comes out to be $\mathcal{M} = 1.22418 M_\odot$.

Once we know the chirp mass we can find the distance using the amplitude expression. The amplitude at time $t = 500$ sec is 110×10^{-21} the corresponding frequency of the wave is $F = 13$ Hz, and substituting the chirp mass value $\mathcal{M} = 1.22526 M_\odot$, in the equation

$$D = \frac{4 \mathcal{M}^{5/3} \pi^{2/3} F(t)^{2/3}}{A(t)} \quad (5.13)$$

The distance comes out to be 8381.67 pc. The amplitude at time $t = 900$ sec is 170×10^{-21} the corresponding frequency of the wave is $F = 24$ Hz, and substituting the chirp mass value $\mathcal{M} = 1.22309 M_\odot$ the distance comes out to be 8137.72 pc. The average distance comes out to be 8259.7 pc.

Table 5.4: Data analysis of inspiral waveform using Newtonian chirp

Time (s)	Instantaneous $F(t)$	Chirp mass M_{\odot}	Instantaneous $A(t)$	Distance (pc)
500	13	1.22526	110×10^{-21}	8381.67
900	24	1.22418	170×10^{-21}	8137.72
		Average = 1.22418	Average = 8259.7	
		Used in code = 1.22	Used in code = 8000	

The data analysis using Newtonian chirp gives chirp mass and distance well in agreement with the values used in code for getting the waveform. If we receive a monochromatic waveform, in which frequency remains constant. Let at some time t we have $F(t) = f_0$

$$f_0 = f_0 \left(1 - \frac{t}{\frac{5}{256(\pi f_0)^{8/3} \mathcal{M}^{5/3}}} \right)^{-3/8}$$

the chirp mass cannot be determined for a monochromatic signal using Frequency expression. The amplitude formula can be used, by knowing instantaneous frequency and amplitude we can substitute to get,

$$\frac{D}{\mathcal{M}^{5/3}} = \frac{4\pi^{2/3} F(t)^{2/3}}{A(t)}$$

There exists degeneracy between distance and mass. If any one of these values we assume or determine via electromagnetic spectrum we can find the other.

Chapter 6

Gravitational waves from accreting millisecond pulsars

Neutron stars possess magnetosphere and they spin rapidly. Neutron stars emit radio beams which if lie along the line of sight of earth we receive radio pulses hence we call them as pulsars. A spherically symmetric rotating object doesn't produce gravitational waves because its quadrupole moment is zero. All stars spin about their axis but neutron stars spin so rapidly that even for a small quadrupole asymmetry detectable emission of gravitational waves occurs. Deformations or internal mechanisms can give rise to quadrupole moment in neutron stars. In a binary system when a neutron star accretes matter from the companion it experiences a spin-up which makes them spin fast. It has been suggested by Bildsten [22] that accretion torque may be balanced by gravitational wave torque which causes no further spin up beyond a stage, which is motivated by electromagnetic spectrum observation that all accreting neutron stars have spin values much less than the break up limit. We choose accreting millisecond pulsar binary as accreting neutron star sources for this study.

6.1 Neutron star spin down and spin up

A spinning neutron star tends to slow down with emission of energy due to the friction in magnetosphere. The period change due to magnetic braking is given by [17]

$$P\dot{P} = \frac{8\pi^2 R^6 B^2 \sin^2 \alpha}{3c^3 I}$$

where P is the period, R is the radius, B is the magnetic field, α is the inclination angle and I is the moment of inertia of the neutron star.

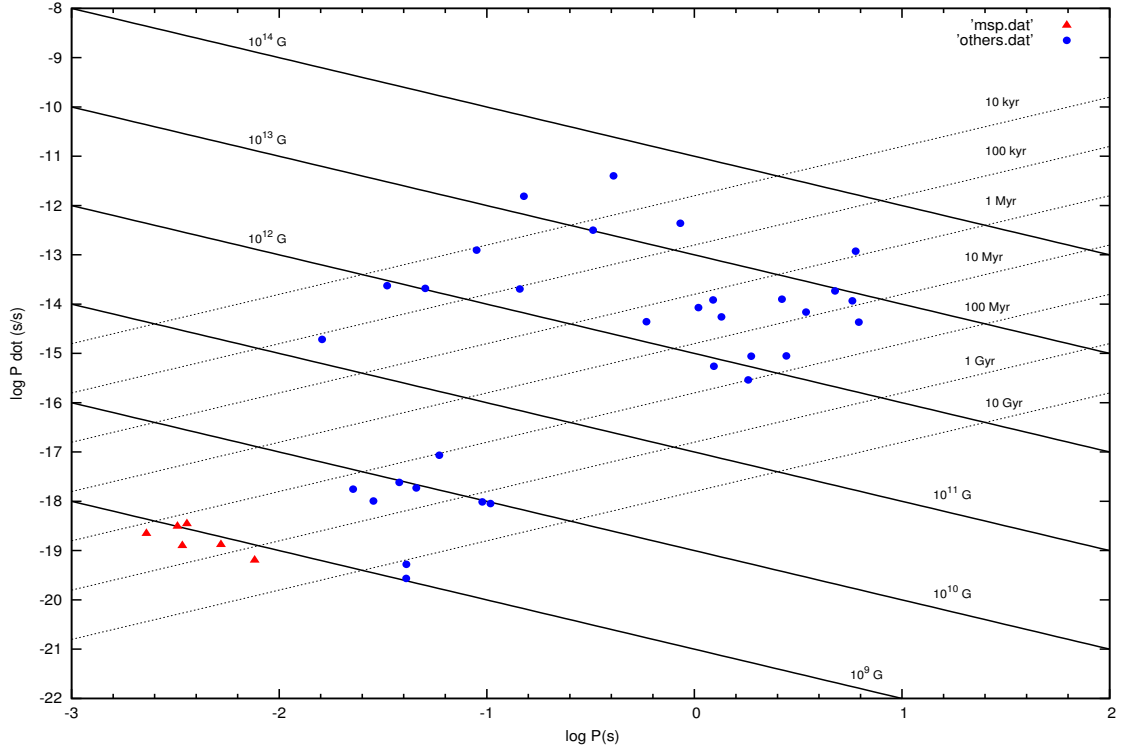


Figure 6.1: P-P dot diagram indicating millisecond pulsars and other pulsars

New born pulsars in general start their lives with strong magnetic fields and moderate spin periods (exception being magnetars which have large magnetic field, large \dot{P} and large P), hence they find a place in P-P dot diagram at top and as their age passes they move downwards due to decrease in their magnetic field and \dot{P} . As the neutron star evolves with time the magnetic fields become weak and spin period becomes quite long such that it cannot emit radio pulses, this situation corresponds to lower-right region of P-P dot diagram called as graveyard and they become radio quiet. Those pulsars which are present in a binary system can come out of graveyard region to the lower-middle and lower-left region of P-P dot diagram and again re-emit radio pulses. This is because the matter gets accreted onto the neutron star from their companions due to Roche lobe overflow and stellar-wind mass transfer, this accreted matter imparts angular momentum which causes spin-up and spin of neutron star decreases and they move to left from graveyard region(lower-right).

The millisecond pulsars lies at bottom left as we see in figure [6.1], indicating that they posses a weak magnetic field of the order 10^9 Gauss and their \dot{P} is of the order 10^{-19} .

The magnetic fields of neutron stars funnel the mass leaked from companion onto the neutron star at its magnetic polar caps, the polar caps gets heated up and can even emit X-rays. And as the neutron star rotates , we receive pulses of X-rays whenever it the X-ray beam emerging from neutron star lies along our line of sight. Observational evidences exist for X-ray pulsars.

The Alfven radius and co-rotation radius governs whether any matter will be accreted onto the neutron star or not. The expressions of Alfven radius and co-rotation radius expressions

are [18, 19]-

$$r_a = \left(\frac{B^2 R^6}{\dot{M} \sqrt{2GM}} \right)^{2/7} \quad (6.1)$$

$$r_{co} = \left(GM \frac{P^2}{4\pi^2} \right)^{1/3} \quad (6.2)$$

where \dot{M} is the mass accretion rate. For a given accretion rate and magnetic field the Alfven radius doesn't change. But change in period causes co-rotation radius to either increase or decrease.

If Alfven radius is smaller than co-rotation radius the in falling matter can get accreted onto the neutron star [18]. The in falling matter from companion star carries angular momentum which is imparted to the neutron star and it spins up and its spin period decreases. The decrease of spin period causes r_{co} to decrease and at one stage when r_{co} becomes smaller than Alfven radius the accretion stops and neutron-star doesn't spin-up any further.

If Alfven radius is greater than co-rotation radius then neutron star doesn't accrete material, and spinning without accreting causes it to spin down due to magnetosphere. Hence its period increases and at a stage when r_{co} becomes greater than Alfven radius it starts to spin-up.

For a accreting neutron star there exists spin-down scenario and spin-up scenario bridged between a equilibrium situation where there is no-spin up or spin-down which happens at $r_a = r_{co}$ and the corresponding spin period is called equilibrium spin period [19],

$$P_{eq} = 2.4 B^{6/7} M^{-5/7} \dot{M}^{-3/7} R^{16/7} \quad (6.3)$$

where B is magnetic field expressed in 10^9 Gauss, M is Mass of the neutron star expressed in solar mass, \dot{M} is the accretion rate expressed in Eddington limit (\dot{M}_{Edd}) and R is the radius of the neutron star expressed in 10^6 cm.

All the accreting pulsars will have a period greater then their P_{eq} . It is the minimum spin period attainable and the corresponding spin frequency is the maximum possible value. By taking $\dot{M} = \dot{M}_{Edd}$, $M = 1.4$ solar mass and $R = 10^6$ cm we get the spin-up line. We plot AMXP sources[24] listed in table 6.2 in logB-logP diagram.

Table 6.1: Accreting Millisecond X-ray pulsars

Source	Magnetic field B	Spin period (P)
	Gauss 10^8	ms
IGR J00291+5934	< 3	1.67
Aql X-1	< 10	1.82
XTE J1751-305	3-7	2.30
SAX J1808.4-3658	1-5	2.49
XTE J1814-338	< 8	3.18
XTE J0929-314	< 30	5.41
SWIFT J1756.9-2508	0.4-9	5.49

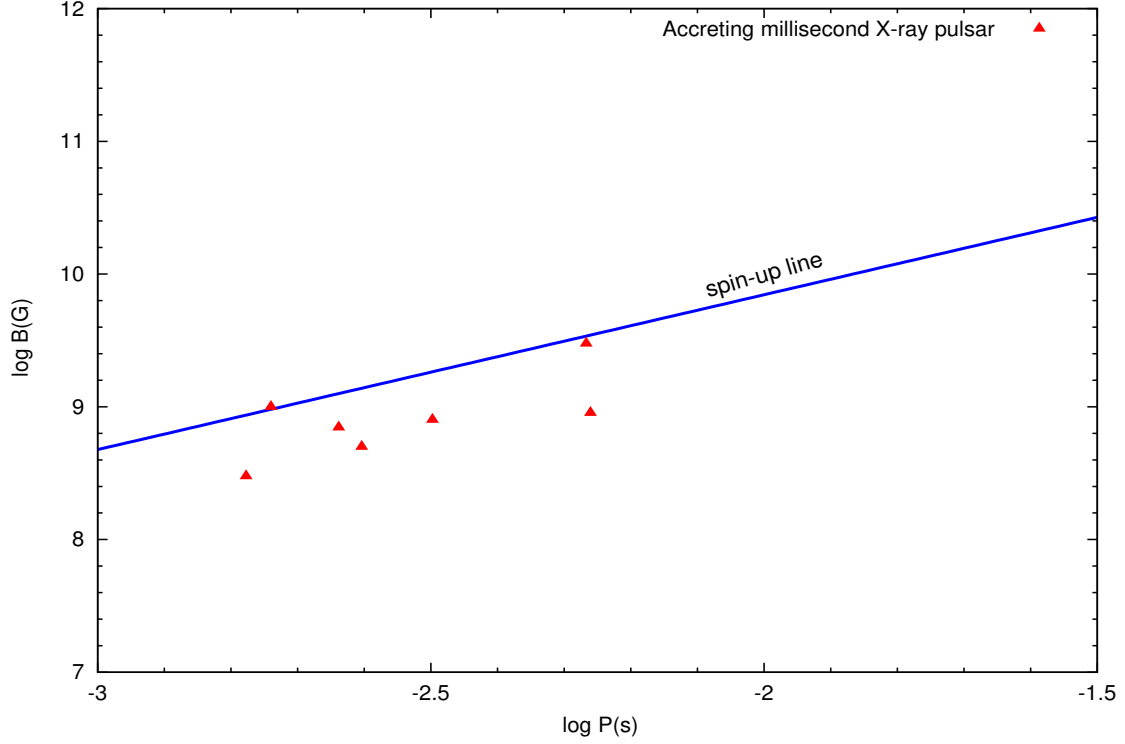


Figure 6.2: The LogB-LogP plot of various accreting x-ray pulsars

Since magnetic field values are uncertain for some of AMXP we have taken the upper limit. We can see that most AMXP lie below the spin-up line and some lie close to spin-up line.

A novel idea proposed by Bildsten [22] suggests that the internal mechanisms or deformations can lead to quadrupole moment in neutron stars, wherein the gravitational wave emitted remains negligible at lower spin value and becomes dominant after a certain spin value and at one stage it balances the torque of accreting matter. Hence instead of spin-up to reach large spin values the gravitational wave emission causes accreting neutron spin to get restricted at certain value. We will describe this idea and analyze few sources in next section.

6.2 Quadrupole asymmetry

We start with obtaining the expression for gravitational wave amplitude due to a spinning star [20][21]. Consider a neutron star spinning with angular frequency ω about the axis passing through it. Two frames can be associated with an rotating object, namely body-fixed frame and space-fixed frame. Taking the axis of body-fixed frame to be X'_1, X'_2, X'_3 and space-fixed frame to be X_1, X_2, X_3 . Assuming that origin of both frames lie at centre of mass of star and orientation is such that $X'_3 = X_3$, we have the two frames related to each other as

$$\begin{bmatrix} X'_1 \\ X'_2 \\ X'_3 \end{bmatrix} = \begin{bmatrix} \cos\omega t & \sin\omega t & 0 \\ -\sin\omega t & \cos\omega t & 0 \\ 0 & 0 & 1 \end{bmatrix} \begin{bmatrix} X_1 \\ X_2 \\ X_3 \end{bmatrix} \quad (6.4)$$

Where the transformation matrix

$$R = \begin{bmatrix} \cos\omega t & \sin\omega t & 0 \\ -\sin\omega t & \cos\omega t & 0 \\ 0 & 0 & 1 \end{bmatrix}$$

is a rotation matrix. The inverse transformation matrix is given by the transpose of it,

$$R^T = \begin{bmatrix} \cos\omega t & -\sin\omega t & 0 \\ \sin\omega t & \cos\omega t & 0 \\ 0 & 0 & 1 \end{bmatrix}.$$

The inertia tensor is given by,

$$I_{ij} = \int \rho(X) [X_K X_K \delta_{ij} - X_i X_j] dX \quad (6.5)$$

where it has a total of 9 components,

$$I = \begin{bmatrix} I_{11} & I_{12} & I_{13} \\ I_{21} & I_{22} & I_{23} \\ I_{31} & I_{32} & I_{33} \end{bmatrix}$$

It can be diagonalized so that it posses only diagonal components as non-zero and all off-diagonal components going to zero. This happens in body-fixed frame where

$$I' = \begin{bmatrix} I_1 & 0 & 0 \\ 0 & I_2 & 0 \\ 0 & 0 & I_3 \end{bmatrix}$$

The inertia tensor of both frames are related by

$$I = R^T I' R \quad (6.6)$$

$$\begin{aligned} \begin{bmatrix} I_{11} & I_{12} & I_{13} \\ I_{21} & I_{22} & I_{23} \\ I_{31} & I_{32} & I_{33} \end{bmatrix} &= \begin{bmatrix} \cos\omega t & -\sin\omega t & 0 \\ \sin\omega t & \cos\omega t & 0 \\ 0 & 0 & 1 \end{bmatrix} \begin{bmatrix} I_1 & 0 & 0 \\ 0 & I_2 & 0 \\ 0 & 0 & I_3 \end{bmatrix} \begin{bmatrix} \cos\omega t & \sin\omega t & 0 \\ -\sin\omega t & \cos\omega t & 0 \\ 0 & 0 & 1 \end{bmatrix} \\ &= \begin{bmatrix} \cos\omega t & -\sin\omega t & 0 \\ \sin\omega t & \cos\omega t & 0 \\ 0 & 0 & 1 \end{bmatrix} \begin{bmatrix} I_1 \cos\omega t & I_1 \sin\omega t & 0 \\ -I_2 \sin\omega t & I_2 \cos\omega t & 0 \\ 0 & 0 & I_3 \end{bmatrix} \\ &= \begin{bmatrix} I_1 \cos^2\omega t + I_2 \sin^2\omega t & I_1 \sin\omega t \times \cos\omega t - I_2 \cos\omega t \times \sin\omega t & 0 \\ I_1 \sin\omega t \times \cos\omega t - I_2 \cos\omega t \times \sin\omega t & I_1 \sin^2\omega t + I_2 \cos^2\omega t & 0 \\ 0 & 0 & I_3 \end{bmatrix} \end{aligned}$$

Therefore the non-zero components of the inertia tensor is

$$\begin{aligned} I_{11} &= I_1 \cos^2 \omega t + I_2 \sin^2 \omega t \\ &= \frac{I_1 + I_2}{2} + \frac{(I_1 - I_2)}{2} \cos 2\omega t \end{aligned}$$

$$\begin{aligned} I_{12} &= I_1 \sin \omega t \times \cos \omega t - I_2 \cos \omega t \times \sin \omega t \\ &= \frac{(I_1 - I_2)}{2} \sin 2\omega t \end{aligned}$$

$$\begin{aligned} I_{21} &= I_1 \sin \omega t \times \cos \omega t - I_2 \cos \omega t \times \sin \omega t \\ &= \frac{(I_1 - I_2)}{2} \sin 2\omega t \end{aligned}$$

$$\begin{aligned} I_{22} &= I_2 \cos^2 \omega t + I_1 \sin^2 \omega t \\ &= \frac{I_1 + I_2}{2} - \frac{(I_1 - I_2)}{2} \cos 2\omega t \end{aligned}$$

$$I_{33} = I_3$$

The quadrupole moment tensor is given by,

$$\mathcal{I}_{\alpha\beta} = \int \rho(X) X_\alpha X_\beta d^3X \quad (6.7)$$

The formula of Inertia tensor in Eq.(6.5) and Quadrupole moment in Eq.(6.7) suggests that

$$\ddot{\mathcal{I}}_{\alpha\beta} = -\ddot{I}_{\alpha\beta} \quad (6.8)$$

Thus we can obtain the components of reduced quadrupole moment tensor as,

$$Q_{\alpha\beta} = \mathcal{I}_{\alpha\beta} - \frac{1}{3} \delta_{\alpha\beta} \mathcal{I} \quad (6.9)$$

$$\ddot{Q}_{\alpha\beta} = \ddot{\mathcal{I}}_{\alpha\beta} - \frac{1}{3} \delta_{\alpha\beta} \ddot{\mathcal{I}} \quad (6.10)$$

The reduced quadrupole tensor comes out to be,

$$\ddot{Q} = 4\omega^2 \begin{bmatrix} -\frac{(I_1 - I_2)}{2} \cos 2\omega t & -\frac{(I_1 - I_2)}{2} \sin 2\omega t & 0 \\ -\frac{(I_1 - I_2)}{2} \sin 2\omega t & \frac{(I_1 - I_2)}{2} \cos 2\omega t & 0 \\ 0 & 0 & 0 \end{bmatrix} \quad (6.11)$$

Taking one more derivative we get

$$\ddot{Q} = 8\omega^3 \begin{bmatrix} \frac{(I_1-I_2)}{2}\sin 2\omega t & -\frac{(I_1-I_2)}{2}\cos 2\omega t & 0 \\ -\frac{(I_1-I_2)}{2}\cos 2\omega t & -\frac{(I_1-I_2)}{2}\sin 2\omega t & 0 \\ 0 & 0 & 0 \end{bmatrix} \quad (6.12)$$

The strain is given by Eq.(3.17),

$$h_{ij} = \frac{2}{D}\ddot{Q}_{ij}$$

$$h = \frac{4\omega^2}{D} \begin{bmatrix} -(I_1 - I_2)\cos 2\omega t & -(I_1 - I_2)\sin 2\omega t & 0 \\ -(I_1 - I_2)\sin 2\omega t & (I_1 - I_2)\cos 2\omega t & 0 \\ 0 & 0 & 0 \end{bmatrix} \quad (6.13)$$

It is clear that only if $I_1 \neq I_2$ components of quadrupole moment derivative are non zero. This happens when there is asymmetry, a spherically symmetric rotating star however fast rotating cannot result in gravitational waves.

$$h = \frac{4\omega^2}{D}(I_1 - I_2)\cos 2\omega t \begin{bmatrix} -1 & 0 & 0 \\ 0 & 1 & 0 \\ 0 & 0 & 0 \end{bmatrix} + \frac{4\omega^2}{D}(I_1 - I_2)\sin 2\omega t \begin{bmatrix} 0 & -1 & 0 \\ -1 & 0 & 0 \\ 0 & 0 & 0 \end{bmatrix}$$

The two polarization comes out to be,

$$h_+ = \frac{4\omega^2}{D}(I_1 - I_2)\cos 2\omega t$$

$$h_\times = \frac{4\omega^2}{D}(I_1 - I_2)\sin 2\omega t$$

Its evident that the gravitational wave frequency is twice the frequency of binary. Which implies that $\omega = \frac{1}{2}\omega_{gw} = \pi F$ where F is the gravitational wave frequency. The gravitational wave amplitude is given by,

$$h_o = \frac{4\omega^2}{D}(I_1 - I_2) \quad (6.14)$$

The total power radiated is,

$$\begin{aligned} \frac{dE}{dt} &= -\frac{1}{5}\ddot{Q}_{\beta\gamma}\ddot{Q}^{\beta\gamma} \\ &= -\frac{1}{5}\left(\ddot{Q}_{xx}^2 + 2\ddot{Q}_{xy}^2 + \ddot{Q}_{yy}^2\right) \\ &= -\frac{1}{5}\frac{(I_1 - I_2)^2}{4} \times 2(8\omega^3)^2 \\ &= -\frac{32}{5}(I_1 - I_2)^2\omega^6 \end{aligned} \quad (6.15)$$

In literature a term $\varepsilon = \frac{I_1 - I_2}{I_3}$ called ellipticity is considered. The value of ellipticity depends on the Neutron star properties. Generally it depends upon maximum strain that can be supported by its crust. Rewriting gravitational wave polarizations and energy radiated using ellipticity we get

$$h_o = \frac{4\omega^2}{D}(I_1 - I_2) = \frac{4\omega^2}{D}\varepsilon I_3 \quad (6.16)$$

$$\frac{dE}{dt} = -\frac{32}{5}\varepsilon^2 I_3^2 \omega^6 \quad (6.17)$$

6.3 Accretion torque and GW torque equilibrium

We can substitute for I_3 from Eq.(6.17) in Eq.(6.16) to get

$$h_o = \frac{4\omega^2}{D}I_3 = \frac{4\omega^2\varepsilon}{D} \left[\frac{5\dot{E}}{32\omega^6\varepsilon^2} \right]^{1/2}$$

$$h_o^2 = \frac{5\dot{E}}{2D^2\omega^2} \quad (6.18)$$

These expressions can be expressed in terms of gravitational wave frequency using $\omega = \pi F$.

Without going into the detail of quadrupole asymmetry whether its internal mechanism or deformations, here we are interested in its affect in the form of gravitational wave radiated away with \dot{E} .

All accreting neutron stars have magnetic field and accreting torque at magnetosphere must be equated to gravitational wave torque, but it has been shown that the value of magnetosphere radius is of the same order as that of the neutron star radius[21]. Hence we can equate spin up torque at Neutron star radius with gravitational wave torque for spin equilibrium.

Accreting matter spin up the neutron star due to accreting torque, $N_a = \dot{M}(MR)^{1/2}$. Luminosity of X-rays, $L = F \times 4\pi D^2$ where F is the flux. Assuming accretion at Eddington limit we get the luminosity is $L = \frac{M\dot{M}}{R}$. Equating we get ,

$$\dot{M} = \frac{4\pi D^2 F R}{M} \quad (6.19)$$

The gravitational wave torque is,

$$N_{gw} = \frac{\dot{E}}{\omega}$$

If accreting torque is balanced by gravitational wave torque the pulsar doesn't spin up further. At this stage,

$$\dot{M}(MR)^{1/2} = \frac{\dot{E}}{\omega}$$

We get

$$\dot{E} = \dot{M}(MR)^{1/2}\omega = \frac{4\pi D^2 F R}{M}(MR)^{1/2}\omega$$

Substituting the above in Eq.(6.18) we get

$$h_o^2 = \frac{5}{2D^2\omega^2} \times \frac{4\pi D^2 F R}{M} (MR)^{1/2} \omega$$

Taking square root we get

$$h_0 = \sqrt{10\pi} F^{1/2} R^{3/4} \omega^{-1/2} M^{-1/4} \quad (6.20)$$

We can express it as [23]

$$h_0 = 3 \times 10^{-27} F^{1/2} \left(\frac{R}{10km} \right)^{3/4} \left(\frac{M}{1.4M_\odot} \right)^{-1/4} \left(\frac{\nu}{1kHz} \right)^{-1/2} \quad (6.21)$$

where R is in km, F is in $10^{-8} \text{erg cm}^{-2} \text{s}^{-1}$, M is in M_\odot and ν is in kHz..

The strain amplitude depends upon radius of neutron star, mass of the neutron star, flux and spin-frequency. We take source parameters from [23] listed in table 6.2. Due to uncertainties in mass and radius values for some sources we assume the value of mass to be $1.4 M_\odot$ and radius to be 10 km.

Table 6.2: Accreting Millisecond X-ray pulsar GW signal

Source	Flux $10^{-8} \text{erg cm}^{-2} \text{s}^{-1}$	Spin Frequency Hz	GW frequency Hz	Strain amplitude h_0
IGR J00291+5934	1.8×10^{-3}	598.892	1197.6	1.64481×10^{-28}
Aql X-1	1.2×10^{-1}	550.274	1100.55	1.40095×10^{-27}
SAX J1748.9-2021	9.2×10^{-3}	442.361	884.722	4.32641×10^{-28}
XTE J1751-305	2×10^{-3}	435.318	870.636	2.03345×10^{-28}
SAX J1808.4-3658	8.6×10^{-3}	400.975	801.95	4.39351×10^{-28}
HETE J1900.1-2455	1.8×10^{-2}	377.296	754.592	6.55264×10^{-28}
XTE J1814-338	1.3×10^{-3}	314.357	628.714	1.92922×10^{-28}
XTE J1807-294	1.4×10^{-3}	190.624	381.248	2.57097×10^{-28}
XTE J0929-314	2.7×10^{-3}	185.105	370.21	3.62321×10^{-28}
SWIFT J1756.9-2508	1.4×10^{-4}	182.066	364.132	8.31899×10^{-29}

Since h_0 is small for all the AMXP sources it is difficult to detect them in gravitational wave detectors. The sources are monochromatic that is their spin frequency remains constant over a longer period of time.

The amplitude spectral density for monochromatic source is given by

$$h_f = h_0 \sqrt{T_{obs}}$$

by choosing the observation time to be 2 years we can detect the gravitational wave signal due to few of these sources with help of data analysis. The amplitude spectral densities of AMXP sources is plotted along with aLIGO in figure [6.3].

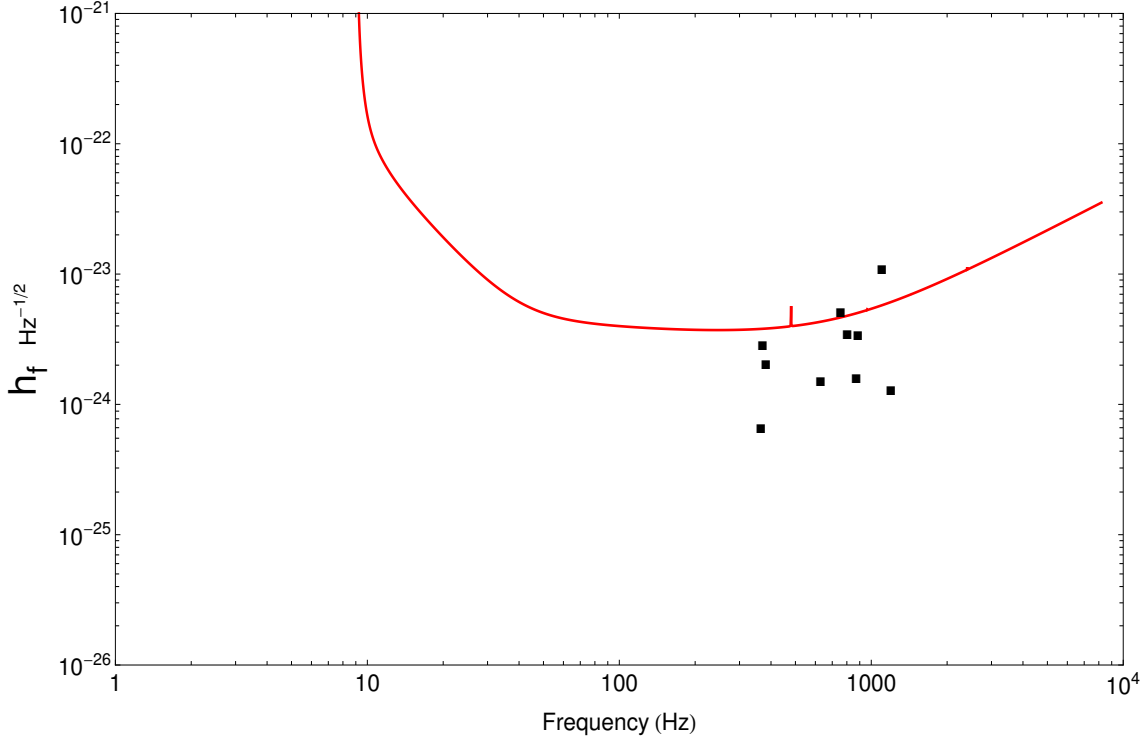


Figure 6.3: AMXP sources and aLIGO sensitivity curve

Sources lying above detector sensitivity curves are detectable. Sources Aql X-1 and HETE J1900.1-2455 can possibly be detected in aLIGO with observation time of 2 years and use of sophisticated data analysis. Future Einstein telescope and cosmic explorer can detect more sources. If all parameters of AMXP sources is well known from electromagnetic observations without any uncertainty, then by creating a single gravitational wave template and using matched filtering the gravitational wave signal from these systems can be pulled out of the noise. Two years of continuous run of detectors, storing the detector data and exact binary parameters values for creating a gravitational wave template are the difficulties which if resolved detection of the gravitational wave signal from AMXP sources can be seen in their respective GW frequency mentioned in the table [6.2] . Also more theoretical and observational developments on the gravitational wave and accretion torque equilibrium also necessary to check the validity of this scenario. The possibility of accreting neutron star systems as sources of detectable gravitational waves where accretion has a crucial role to play remains an interesting idea for future gravitational wave astronomy.

Conclusion

Binary stars are continuous sources of gravitational waves. In leading order the gravitational waves produced from binaries in circular orbit has frequency twice the orbital frequency and is called as Newtonian chirp. Newtonian chirp (the leading order Post-Newtonian approximation) is based upon the assumption that masses are point objects, which is not true for real systems but still is a good approximation. The amplitude spectral density of Newtonian chirp is used to determine whether the inspiral phase of a binary can be observed in ground base detectors and hence the study of it for binaries with the aLIGO and LIGO sensitivity curves helps us to understand the detector's capabilities and the possible developments that could be made to make the detectors more efficient. Einstein telescope and Cosmic explorer are advanced interferometer detectors for the future.

Spinning neutron stars with quadrupole asymmetry can produce gravitational waves. For neutron stars asymmetry arises in them due to internal mechanisms and the gravitational wave emission occurs. The gravitational waves emitted has frequency twice the value of spin frequency of neutron star. If the neutron stars are accreting then they spin-up, there can exist a situation where accretion torque is balanced by gravitational torque and they attain a spin-equilibrium even though accretion continues to happen.

Though gravitational waves due to orbital motion of known binary stars are not possible to be seen in aLIGO detectors due to lowest observable frequency limit (10 Hz), but aLIGO can detect gravitational waves due to orbital motion from unseen binaries located at cosmic distances which have reached the late inspiral phases. The gravitational waves from spinning neutron star in some of the known AMXP binary can be detectable in aLIGO.

This study brings out the essential features of GW produced by orbital motion of different compact binary systems and the possibilities of detecting them ; which helps us to understand the insights which Newtonian chirp convey regarding the actual inspiral gravitational wave signals which are complex in nature. This study also presents the gravitational wave torque and accretion torque balance scenario which is motivated with electromagnetic observation of accreting neutron stars, and brings out few sources which could be observed in gravitational wave regime.

Bibliography

- [1] Tai L Chow, *Mathematical Methods for Physicists*, Cambridge University Press; 1 edition (July 31, 2000)
- [2] Jayant Narlikar, *An Introduction to Relativity*, Cambridge University Press; 1 edition (February 26, 2010)
- [3] M. P. Hobson, G. P. Efstathiou & A. N. Lasenby, *General Relativity: An Introduction for Physicists*, Cambridge University Press; 1 edition (February 2, 2006)
- [4] Sean Carroll, *Lecture Notes on General Relativity*, arXiv:gr-qc/9712019
- [5] Jeroen Burgers, *Gravitational Waves in Astrophysics* (2009)
- [6] Cole Miller, *Overview of Gravitational Radiation & Gravitational Wave Sources*, 2014 Winter School on Compact Objects
- [7] General Relativity course lecture notes, Utah State State University (2013).
- [8] T. Padmanabhan, *Gravitation : Foundations and Frontiers*, Cambridge University Press; 1 edition (February 2, 2006)
- [9] P. Ajith, S. Mohapatra, and A. Pai, *A Gravitational Wave Data Analysis Primer for the IndiGO Mock Data Challeng*
- [10] P. Ajith, A. Ghosh, *A Tutorial on GW Data Analysis*
- [11] Katherine Grover, *Physics and Astrophysics with Gravitational Waves from Compact Binary Coalescence in Ground Based Interferometers*, PhD thesis, University of Birmingham, October 2015
- [12] Tjonnie G.F.Li, *Extracting physics from Gravitational Waves*, PhD thesis, VU University Amsterdam, October 2013
- [13] G. Srinivasan, *The Maximum Mass of Neutron Stars*, Bull.Astr.Soc.India (2002) **30**, 523-547.
- [14] Cutler and Thorne, *An overview of Gravitational wave sources*, arXiv:gr-qc/0204090.

- [15] B.P. Abbott et al., *Observation of Gravitational Waves from a Binary Black Hole Merger*, Physics Review Letters **116**, 061102 (2016).
- [16] C.J. Moore, R.H. Cole and C.P.L. Berry, *Gravitational-wave sensitivity curves*, Classical & Quantum Gravity, 32(1):015014 (2015), arXiv:1408.0740v2 [gr-qc].
- [17] D. Lorimer and M. Kramer, *Handbook of Pulsar Astronomy*, Cambridge University Press (2005)
- [18] E. P. J. van den Heuvel, *Evolutionary processes in X-ray binaries and their progenitor systems*, Annals New York Academy of Sciences(1977)
- [19] D. Battacharya and E. P. J. van den Heuvel, *Formation and evolution of binary and millisecond pulsars*, Phys. Rep.203(1991)
- [20] Alessandra Buonanno, *Gravitational Waves*, Lectures given at the Fabric of Spacetime Summer School (2006),arXiv:0709.4682v1
- [21] Alessandro Mion, *A Search for Gravitational Waves from Pulsars in Binary Systems Using Auriga & Radiotelescope Observations*, University of Toronto PhD thesis (2006-2007)
- [22] L. Bildsten, *Gravitational Radiation and Rotation of Accreting Neutron Stars*, The Astrophysical Journal, Volume 501, L89 (1998)
- [23] Watts et al., *Detecting gravitational wave emission from the known accreting neutron stars*, Mon.Not.Roy.Astron.Soc.389:839-868,(2008)
- [24] Sushan Konar, *The magnetic fields of millisecond pulsars in globular clusters*, Mon.Not.Roy.Astron.Soc.409:259-268,(2010)